Excem Research Papers in Electronics and Electromagnetics

Number 9 June 2024 ISBN 978-2-909056-29-6

# Some Mathematical Models of a Circular Wire Loop Antenna

**FRÉDÉRIC BROYDÉ[1], and EVELYNE CLAVELIER[2]**

[1]Eurexcem, 12 chemin des Hauts de Clairefontaine, 78580 Maule, France
[2]Excem, 12 chemin des Hauts de Clairefontaine, 78580 Maule, France

Corresponding author: Frédéric Broydé (e-mail: fredbroyde@eurexcem.com).

**ABSTRACT** We investigate a single-turn circular wire loop antenna lying in a homogeneous and lossless medium, in the framework of known explicit mathematical models of the current distribution in the loop antenna and the impedance presented by the loop antenna. We obtain improved equivalent formulas and approximate formulas for these models. We derive mathematical models about emission by the loop antenna. These models include new approximate but accurate formulas for the computation of the vector effective length. We obtain new mathematical models and results about reception by the loop antenna.

**INDEX TERMS** Antenna theory, loop antenna, measuring antenna, electromagnetic compatibility, EMC.

## I. INTRODUCTION

We consider a single-turn circular wire loop antenna, similar to the one shown in Fig. 1, lying in a homogeneous and lossless medium. This loop antenna is made of a perfect electric conductor (PEC) having a circular cross-section of diameter $d_w$. The center line of the PEC is an arc of a circle of radius $a$. The antenna is used for emission or reception of time-harmonic signals at a radian frequency $\omega$, corresponding to a wavelength $\lambda$ and a wave number $k$ in said medium. We assume that: the wire is sufficiently thin for $d_w \ll 2a$ to hold; and the wire radius is electrically small, that is, $kd_w \ll 1$. We also postulate that the antenna has a narrow gap, each side of the gap being one of the antenna terminals.

This article presents mathematical models which may be used to compute the loop antenna's behaviour as regards emission and reception.

Section II is about a known explicit mathematical model for the current distribution in the loop antenna during emission, and the associated explicit mathematical model of the impedance presented by the loop antenna. These models contain complicated frequency-dependent integrals and special functions of arguments depending on $a$ and $d_w$, so that the effects of the frequency, $a$ and $d_w$ are difficult to grasp. In Section III, we obtain new equations for these models: equivalent formulas without integrals depending on the frequency, and then approximate formulas without special functions of arguments depending on $a$ and $d_w$.

We derive mathematical models which may be used to compute the loop antenna's behaviour, as regards emission in Section IV, and as regards reception in Section V. These models include new approximate but accurate formulas for the computation of the vector effective length, which are found to be useful for estimating the limitations of an electrically small single-turn circular loop antenna used as a probe or a measuring antenna, or in direction finding.

The existing literature relevant to this work is cited and reviewed in the next sections, where it is easier to compare it to our results.

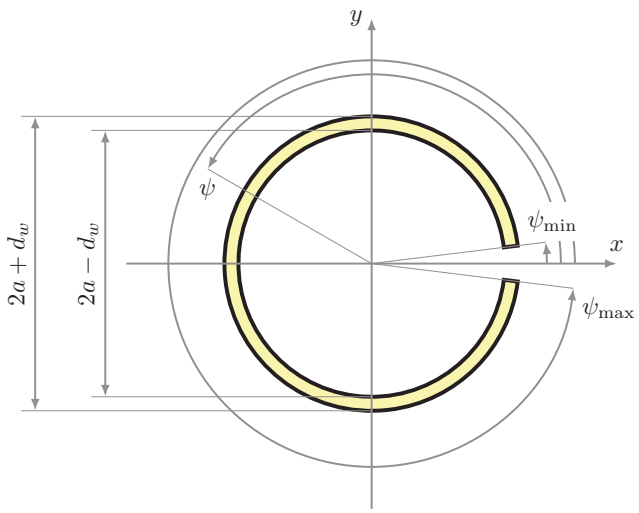


**FIGURE 1.** The single-turn circular loop.

## II. CURRENT DISTRIBUTION AND IMPEDANCE

### A. NOTATIONS AND ASSUMPTIONS

The antenna's positive terminal corresponds to an angle $\psi_{\min} > 0$ shown in Fig. 1, and the antenna's negative terminal to an angle $\psi_{\max} = 2\pi - \psi_{\min}$, also shown in Fig. 1. The physical space between these terminals is the gap. Since we postulate a narrow gap, $\psi_{\min} \ll \pi/18$.

A time factor $e^{j\omega t}$ is assumed and suppressed throughout the paper. In this Section II, the loop antenna is used for emission, and excited by a generator applying a voltage $U_0$ to the gap. Whatever is connected to the antenna ports is regarded as a part of the generator, so that, if an actual setup comprises a feeder (i.e., a feed line), the feeder is a part of the generator. We assume that the generator is equivalent to a perfectly conducting wire, the wire closing the gap in such a way that the wire and the loop antenna form a solid torus, the wire being encircled by some distribution of small loops of impressed magnetic current, of total electromotive force $U_0$, the resulting distribution of impressed magnetic current density being symmetric with respect to the plane $y = 0$. This is a broad assumption [1, Sec 3-1] [2, Appendix III].

At an arbitrary angle $\psi$ such that $0 \leqslant \psi \leqslant 2\pi$, the current $i_E(\psi)$ flowing in the loop antenna or in the gap is positive in the direction of increasing $\psi$, so that $i_E(\psi_{\min})$ is a current flowing into the positive terminal, and $i_E(\psi_{\max})$ a current flowing out of the negative terminal. It follows from our assumptions that the generator does not deliver a common-mode current, that is to say $i_E(\psi_{\max}) = i_E(\psi_{\min})$.

### B. MODEL FOR THE CURRENT DISTRIBUTION

The symmetry of the problem is such that $i_E(\psi)$ is given by a Fourier cosine series

$$i_E(\psi) = \sum_{n=0}^{\infty} I_{E\,n} \cos(n\psi) \tag{1}$$

Wu explained how the current distribution may be computed, in the case of a loop antenna made of a PEC, excited by a delta-gap source [3]. This approach was further developed and implemented by King and other authors in [4]–[5], in [6, Ch. 4] and in [7, Ch. 11]. According to the resulting theory, if the positive integer $N$ is sufficiently large but not too large, $i_E(\psi)$ is accurately given by

$$i_E(\psi) \simeq \frac{V_0}{j\pi\eta} \left\{ \frac{1}{A_0} + 2 \sum_{n=1}^{N} \frac{\cos n\psi}{A_n} \right\} \tag{2}$$

where $V_0$ is the voltage of the delta-gap source and where $\eta$ is the intrinsic impedance of the medium [4], [6, Ch. 4], [7, Sec. 11.4]. The Wu-King factors $A_0, \ldots, A_N$ are

$$A_0 = ka\,\kappa_1 \tag{3}$$

and, for $n \in \{1, \ldots, N\}$,

$$A_n = ka \frac{\kappa_{n+1} + \kappa_{n-1}}{2} - \frac{n^2}{ka} \kappa_n \,, \tag{4}$$

the quantities $\kappa_0$ to $\kappa_{N+1}$ being given by

$$\kappa_0 = \frac{1}{\pi} \ln \frac{16a}{d_w} - \frac{j}{2} \int_0^{2ka} B(x, 0)\, dx \tag{5}$$

and, for $n \in \{1, \ldots, N+1\}$,

$$\kappa_n = \frac{\mathrm{K}_0\left(\frac{nd_w}{2a}\right) \mathrm{I}_0\left(\frac{nd_w}{2a}\right) + C_n}{\pi} - \frac{j}{2} \int_0^{2ka} B(x, 2n)\, dx \,, \tag{6}$$

in which $\mathrm{K}_0$ and $\mathrm{I}_0$ are modified Bessel functions, in which

$$C_n = \ln(4n) + \gamma - 2 \sum_{m=0}^{n-1} \frac{1}{2m+1} \,, \tag{7}$$

where $\gamma$ is Euler's constant, and in which, for any $x \in \mathbb{R}$,

$$B(x, \nu) = \frac{1}{\pi} \int_0^{\pi} e^{j(\nu\phi - x\sin\phi)}\, d\phi \tag{8}$$

where $\nu$ is zero or an even positive integer.

The Wu-King factors are dimensionless. By (2), $i_E(\psi)$ depends on only 3 real variables: $\psi$, $ka$ and $2a/d_w$.

Since $\nu$ is always an integer in (8), we can use results shown in [8, p. 145] and [8, p. 251] to write

$$B(x, \nu) = \mathrm{J}_\nu(x) + j\mathcal{E}_\nu(x) = \mathrm{J}_\nu(x) - j\Omega_\nu(x) \,, \tag{9}$$

where $\mathrm{J}_\nu$ is a Bessel function and $\mathcal{E}_\nu = -\Omega_\nu$ is a Weber function (in [3], [4] and [7], $\Omega_\nu = -\mathcal{E}_\nu$ is called a Lommel-Weber function).

Let $c$ be the velocity of light in the medium. The value $N = 19$, corresponding to 20 terms in (2), provides accurate values up to the frequency

$$f_{\max} = \frac{2.5\,c}{2\pi a} \tag{10}$$

if $2a/d_w > 24$, or up to a lower frequency if the loop antenna is thicker [4], [7]. For any frequency $f \leqslant f_{\max}$, we have $ka \leqslant 2.5$ so that $B(x, \nu)$ can accurately be computed using (8) and a numerical integration. However, we found the computation of the Wu-King factors to be much faster if we use (9), the expansion

$$\mathrm{J}_\nu(x) \simeq \left(\frac{x}{2}\right)^\nu \sum_{p=0}^{15} \frac{\left(\frac{-x^2}{4}\right)^p}{p!(\nu+p)!} \tag{11}$$

based on [9, Eq. 9.1.10] and the fact that $\nu$ is a nonnegative integer, and the expansion

$$\mathcal{E}_\nu(x) \simeq \frac{-x}{2}(-1)^{\nu/2} \sum_{p=0}^{15} \frac{\left(\frac{-x^2}{4}\right)^p}{\Gamma\left(p + \frac{3+\nu}{2}\right) \Gamma\left(p + \frac{3-\nu}{2}\right)} \tag{12}$$

based on [10, Eq. 11.10.9] and the fact that $\nu$ is zero or an even positive integer.

It follows from (1) and (2) that:

$$I_{E\,0} \simeq \frac{V_0}{j\pi\eta\, A_0} \,; \tag{13}$$

for $n \in \{1, \ldots, N\}$, we have

$$I_{E\,n} \simeq \frac{2V_0}{j\pi\eta\, A_n} \,; \tag{14}$$

and, for $n > N$, we have

$$I_{E\,n} \simeq 0 \,. \tag{15}$$

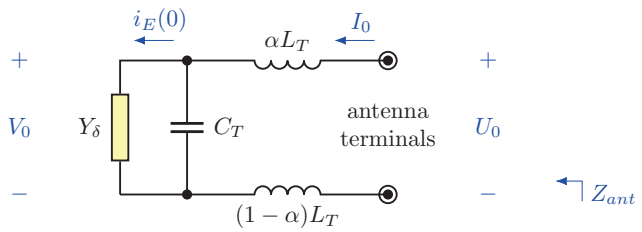


**FIGURE 2.** The terminal-zone network, connected to $Y_\delta$.

### C. TERMINAL-ZONE NETWORK

To obtain a good measure of the impedance of the loop antenna, denoted by $Z_{ant}$, the conventional admittance

$$Y_\delta = \frac{i_E(0)}{V_0} \simeq \frac{1}{j\pi\eta}\left\{\frac{1}{A_0} + 2\sum_{n=1}^{N}\frac{1}{A_n}\right\}, \qquad (16)$$

assumed to exist at the gap of the antenna, should be corrected to take into account the actual configuration close to the gap, by introducing a suitable terminal-zone network in the model, in a manner paralleling that described for dipole antennas [4], [6, Ch. 4], [7, Sec. 11.4]. Terminal-zone networks for dipole antennas have been thoroughly covered in [11, Sec. II.7–II.9], [11, Sec. II.33–II.38] and [12, Sec. 8.1–8.2].

A possible terminal-zone network is shown in Fig. 2, where $\alpha$ is an arbitrary real number. This terminal-zone network comprises a lumped inductance $L_T$ and a lumped capacitance $C_T$ which need not be nonnegative, $C_T$ being connected in parallel with $Y_\delta$ to obtain the admittance $Y_\delta + j\omega C_T$ subject to the voltage $V_0$, this admittance being connected in series with $L_T$ to obtain the impedance $Z_{ant}$ subject to the voltage $U_0$. It follows that we have

$$Z_{ant} \simeq \frac{1}{\dfrac{1}{j\pi\eta}\left\{\dfrac{1}{A_0} + 2\sum\limits_{n=1}^{N}\dfrac{1}{A_n}\right\} + j\omega C_T} + j\omega L_T \qquad (17)$$

and

$$V_0 \simeq \frac{U_0}{1 + \omega L_T\left(\dfrac{1}{\pi\eta}\left\{\dfrac{1}{A_0} + 2\sum\limits_{n=1}^{N}\dfrac{1}{A_n}\right\} - \omega C_T\right)}. \qquad (18)$$

In this model, the current flowing into the positive terminal of the antenna, denoted by $I_0$ and such that $U_0 = Z_{ant} I_0$, is equal to the current flowing out of the negative terminal of the antenna (so that there is no common-mode current flowing into the antenna), but it need not be exactly equal to $i_E(\psi_{\min}) = i_E(\psi_{\max})$. It satisfies

$$I_0 \simeq V_0\left(\frac{1}{j\pi\eta}\left\{\frac{1}{A_0} + 2\sum_{n=1}^{N}\frac{1}{A_n}\right\} + j\omega C_T\right), \qquad (19)$$

so that

$$\frac{i_E(\psi)}{I_0} \simeq \frac{\dfrac{1}{A_0} + 2\sum\limits_{n=1}^{N}\dfrac{\cos n\psi}{A_n}}{\dfrac{1}{A_0} + 2\sum\limits_{n=1}^{N}\dfrac{1}{A_n} - \pi\eta\omega C_T}. \qquad (20)$$

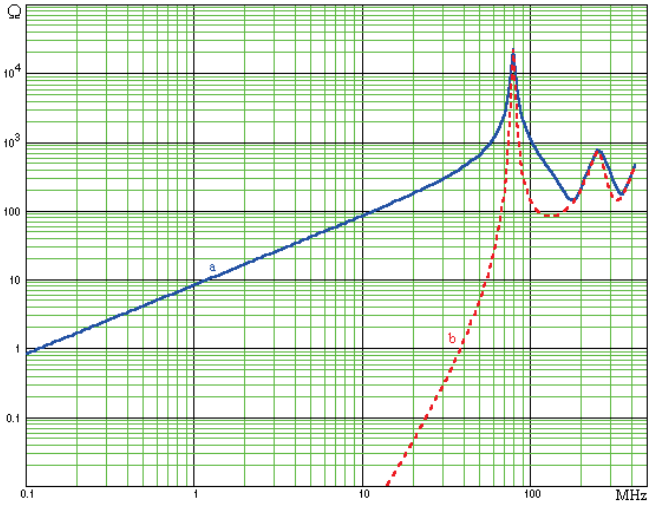


**FIGURE 3.** Impedance of the loop antenna, versus frequency. Absolute value of the impedance: curve "a". Real part of the impedance: curve "b".

### D. EXAMPLES

The mathematical models for $i_E(\psi)$ and $Z_{ant}$ defined by (2)–(18) are easily implemented, and published values of $Y_\delta$ may be used to validate a program. We checked that values of $Y_\delta$ computed by a program based on (2)–(9), (11)–(12) and (16), for $2\ln(4\pi a/d_w) = 12$ and $ka$ in the range 0.05 to 2.00, by utilizing $N = 19$ and the inaccurate value $120\,\pi$ ohms of the intrinsic impedance of vacuum $\eta_0$, are exactly equal to the corresponding values tabulated with 4 decimal places in [4] and [6, Ch. 4]. Slightly different values were obtained when this program used an accurate value of $\eta_0$, as it did to deliver the results shown hereinafter.

We now consider a loop antenna made of a PEC in vacuum, with $a = 280\,\text{mm}$ and $d_w = 14\,\text{mm}$, for which $f_{\max} \simeq 426\,\text{MHz}$. For $C_T = 0\,\text{pF}$, $L_T = 0\,\text{nH}$ and $N = 20$, we study the results computed by said program. Let $\text{Re}(x)$ denote the real part of a complex number $x$. Fig. 3 shows $|Z_{ant}|$ and $\text{Re}(Z_{ant})$ up to about 422 MHz, plotted with 40 points per decade of frequency. According to Fig. 3, the first parallel resonance occurs near 79.3 MHz, the first series resonance near 179 MHz, the second parallel resonance near 256 MHz and the second series resonance near 352 MHz.

Fig. 4 shows seven curves providing information on the Wu-King factors, plotted up to about 422 MHz with 40 points per decade of frequency. Up to about 30 MHz, $|1/A_0|$ is much greater than $|1/A_n|$ for $n \geqslant 1$, so that the contents of the curly brackets in (16) is very close to $|1/A_0|$. Up to about 60 MHz, $|1/A_0|$ has a slope of about $-20$ dB/decade, while $|1/A_1|$ to $|1/A_5|$ have a slope of about 20 dB/decade. We also note that the first series resonance frequency approximately corresponds to a maximum of $|1/A_1|$, and the second series resonance frequency to a maximum of $|1/A_2|$.

Fig. 5 to Fig. 7 show the normalized current distribution $|i_E(\psi)/I_0|$ at different frequencies. At low enough frequencies the current is of course uniform in the loop antenna, so that $|i_E(\psi)/I_0| \simeq 1$. We see that this is accurate at 10 MHz, but no longer at 30 MHz and above.

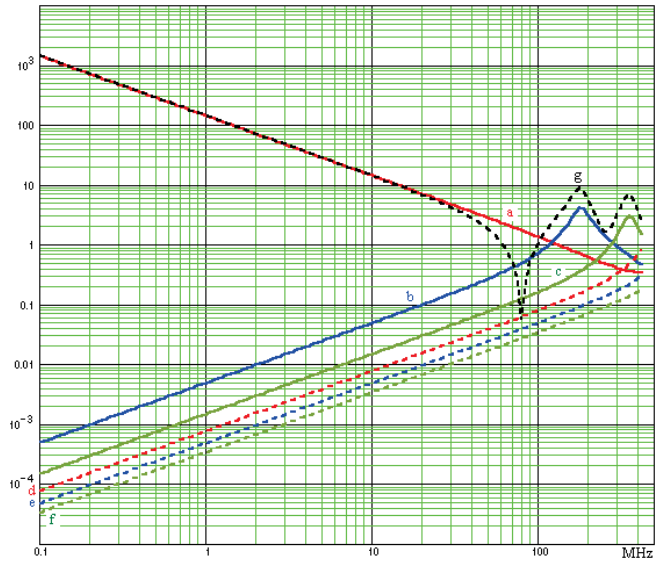


**FIGURE 4.** Information on the Wu-King factors. $|1/A_0|$ is curve "a", $|1/A_1|$ is curve "b", $|1/A_2|$ is curve "c", $|1/A_3|$ is curve "d", $|1/A_4|$ is curve "e", $|1/A_5|$ is curve "f", and the absolute value of the contents of the curly brackets in (16) is curve "g".

### E. DISCUSSION

The current distribution $i_E(\psi)$ and the input current $I_0$ presented in Section II.B and Section II.C are applicable to a lossless circular loop antenna used for emission and subject to the voltage $U_0$, so that, if $I_0 \neq 0\,\mathrm{A}$, its impedance is $Z_{ant} = U_0/I_0$, where $Z_{ant}$ is given by (17). We can also consider the lossless semi-circular loop antenna shown in Fig. 8, which is built over an infinite plane made of a PEC. The current distribution $i_E(\psi)$, where $\psi \in [0, \pi]$, and the input current $I_0$ are applicable to this semi-circular loop antenna used for emission and subject to the voltage $U_0/2$, according to image theory [13, Sec. 2-3], [14, Sec. 5-3]. Thus, the impedance of the semi-circular loop antenna is $Z_{ant}/2$.

An improved computation of the current distribution in a semi-circular loop antenna used for emission, and of the resulting antenna impedance, is proposed by Smith in [15]. In this improved computation, the delta-gap source used in the theory of Wu and King is replaced with a magnetic frill generator. If the antenna feeding configuration accurately corresponds to the one assumed to introduce the magnetic frill generator, the agreement between experiment and theory is excellent, without using a terminal-zone network. However, this semi-circular loop antenna feeding configuration cannot be realized in a circular loop antenna.

In 2006, Anastassiou proposed a new approach to the computation of the current distribution in a circular loop antenna used for emission, and of the resulting antenna impedance. This approach is based on a method of moment formulation, cast in such a way that accurate expressions are obtained at a low computational cost, without the upper frequency limit given by (10). The case of a delta-gap source is covered in [16], and the case of a magnetic frill generator is treated in [17]. The current distributions obtained in this manner are not in the form of the Fourier cosine series (1), though.

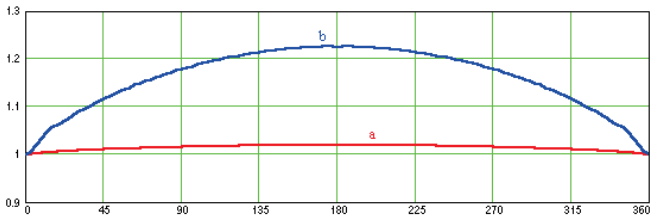


**FIGURE 5.** Normalized current distribution $|i_E(\psi)/I_0|$ versus $\psi$ in degrees: at about 10.0 MHz is curve "a"; and at about 31.6 MHz is curve "b".

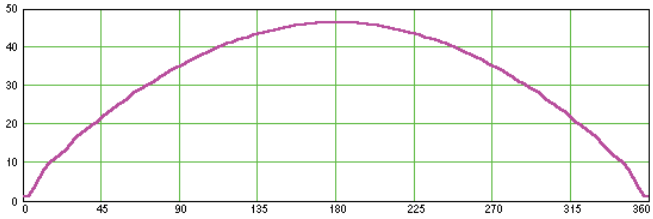

**FIGURE 6.** Normalized current distribution $|i_E(\psi)/I_0|$ versus $\psi$ in degrees, at about 79.4 MHz (near the first parallel resonance, for which $ka \simeq 0.466$).

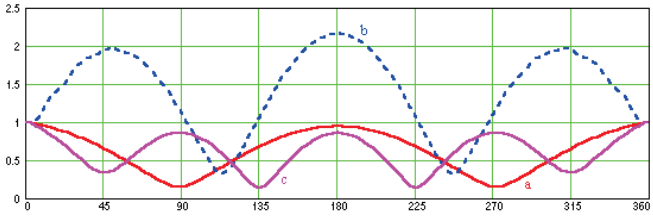


**FIGURE 7.** Normalized current distribution $|i_E(\psi)/I_0|$ versus $\psi$ in degrees: at about 178 MHz (near the first series resonance, for which $ka \simeq 1.048$) is curve "a"; at about 251 MHz (near the second parallel resonance, for which $ka \simeq 1.505$) is curve "b"; and at about 355 MHz (near the second series resonance, for which $ka \simeq 2.063$) is curve "c".

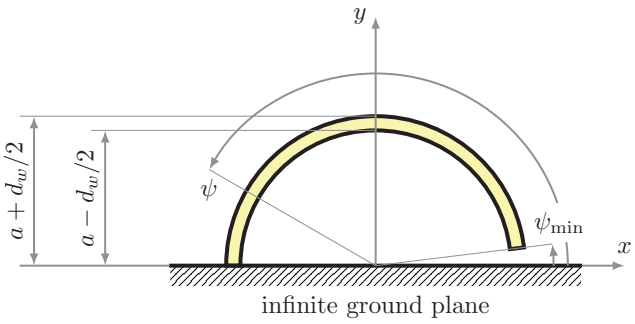


**FIGURE 8.** The semi-circular loop.

## III. ANALYSIS OF THE WU-KING FACTORS

### A. THE FREQUENCY-DEPENDENT INTEGRALS

In (5) and (6), each quantity $\kappa_n$ is a sum of: a first term that only depends on $2a/d_w$ and $n$; and a second term that only depends on $ka$ and $n$, through the frequency-dependent integral

$$-\frac{j}{2}\int_0^{2ka} B(x,2n)\,dx = \frac{1}{2}\int_0^{2ka} \mathcal{E}_{2n}(x)\,dx - \frac{j}{2}\int_0^{2ka} \mathrm{J}_{2n}(x)\,dx\,. \quad (21)$$

We want to exactly compute this frequency-dependent integral, in the form of a power series in the variable $ka$.

According to [10, Eq. 11.10.9], we have

$$\mathcal{E}_\nu(x) = \frac{-x}{2}(-1)^{\nu/2} \sum_{p=0}^{\infty} \frac{\left(\frac{-x^2}{4}\right)^p}{\Gamma\left(p+\frac{3+\nu}{2}\right)\Gamma\left(p+\frac{3-\nu}{2}\right)}, \quad (22)$$

so that

$$\int_0^{2ka} \mathcal{E}_{2n}(x)\,dx = (-1)^{n+1} \sum_{p=0}^{\infty} \frac{(-1)^p \int_0^{2ka} \left(\frac{x}{2}\right)^{2p+1} dx}{\Gamma(p+n+1.5)\,\Gamma(p-n+1.5)}. \quad (23)$$

This leads us to

$$\int_0^{2ka} \mathcal{E}_{2n}(x)\,dx = (-1)^{n+1} \sum_{p=0}^{\infty} \frac{(-1)^p (ka)^{2p+2}}{(p+1)\Gamma(p+n+1.5)\,\Gamma(p-n+1.5)}. \quad (24)$$

According to [9, Eq. 9.1.10], we have

$$\mathrm{J}_\nu(x) = \left(\frac{x}{2}\right)^\nu \sum_{p=0}^{\infty} \frac{\left(\frac{-x^2}{4}\right)^p}{p!(\nu+p)!} \quad (25)$$

so that

$$\int_0^{2ka} \mathrm{J}_{2n}(x)\,dx = \sum_{p=0}^{\infty} \frac{(-1)^p \int_0^{2ka} \left(\frac{x}{2}\right)^{2n+2p} dx}{p!\,(2n+p)!}. \quad (26)$$

This leads us to

$$\int_0^{2ka} \mathrm{J}_{2n}(x)\,dx = 2(ka)^{2n+1} \sum_{p=0}^{\infty} \frac{(-1)^p (ka)^{2p}}{p!\,(2n+p)!(2n+2p+1)}. \quad (27)$$

Using (24) and (27) in (21), we get (28) shown at the bottom of this page. It follows that

$$-\frac{j}{2}\int_0^{2ka} B(x,2n)\,dx = \sum_{q=1}^{\infty} \chi_{q\,n}(ka)^q, \quad (29)$$

where, if $q$ is even, $\chi_{q\,n}$ is real and given by

$$\chi_{q\,n} = \frac{(-1)^{n+\frac{q}{2}}}{q\,\Gamma\left(\frac{q}{2}+n+0.5\right)\Gamma\left(\frac{q}{2}-n+0.5\right)}, \quad (30)$$

and where, if $q$ is odd, $\chi_{q\,n}$ is 0 if $q \leqslant 2n-1$, or imaginary and given by

$$\chi_{q\,n} = -j\frac{(-1)^{\frac{q-1}{2}-n}}{q\left(\frac{q-1}{2}-n\right)!\left(\frac{q-1}{2}+n\right)!} \quad (31)$$

if $q \geqslant 2n+1$.

The coefficients $\chi_{q\,n}$ are dimensionless numbers, which are independent of the frequency and of the characteristics of the antenna. Some approximate values of $\chi_{q\,n}$ are shown in Table 1. We will use the polynomial approximation

$$-\frac{j}{2}\int_0^{2ka} B(x,2n)\,dx \simeq \sum_{q=1}^{d_B(n)} \chi_{q\,n}(ka)^q, \quad (32)$$

of degree less than or equal to $d_B(n)$, resulting from a truncation of the power series in (29). The number $d_B(n)$ of terms which are necessary to obtain a given accuracy in (32) depends on $ka$, hence on the frequency $f$.

$$-\frac{j}{2}\int_0^{2ka} B(x,2n)\,dx = \sum_{p=0}^{\infty} \frac{(-1)^{n+p+1}(ka)^{2p+2}}{2(p+1)\Gamma(p+n+1.5)\,\Gamma(p-n+1.5)} - j\sum_{p=0}^{\infty} \frac{(-1)^p (ka)^{2n+2p+1}}{p!\,(2n+p)!(2n+2p+1)}. \quad (28)$$

**TABLE 1.** Some approximate values of $\chi_{q\,n}$ defined in Section III.A.

| $q$ \ $n$ | 0 | 1 | 2 | 3 | 4 | 5 | 6 |
|---|---|---|---|---|---|---|---|
| 1 | $-1.000000\,j$ | 0 | 0 | 0 | 0 | 0 | 0 |
| 2 | $-6.366198\times10^{-1}$ | $2.122066\times10^{-1}$ | $4.244132\times10^{-2}$ | $1.818914\times10^{-2}$ | $1.010508\times10^{-2}$ | $6.430503\times10^{-3}$ | $4.451887\times10^{-3}$ |
| 3 | $3.333333\times10^{-1}\,j$ | $-1.666667\times10^{-1}\,j$ | 0 | 0 | 0 | 0 | 0 |
| 4 | $1.414711\times10^{-1}$ | $-8.488264\times10^{-2}$ | $1.212609\times10^{-2}$ | $1.347343\times10^{-3}$ | $3.674576\times10^{-4}$ | $1.413297\times10^{-4}$ | $6.595387\times10^{-5}$ |
| 5 | $-5.000000\times10^{-2}\,j$ | $3.333333\times10^{-2}\,j$ | $-8.333333\times10^{-2}\,j$ | 0 | 0 | 0 | 0 |
| 6 | $-1.509025\times10^{-2}$ | $1.077875\times10^{-2}$ | $-3.592916\times10^{-3}$ | $3.266287\times10^{-4}$ | $2.512529\times10^{-5}$ | $5.025057\times10^{-6}$ | $1.477958\times10^{-6}$ |
| 7 | $3.968254\times10^{-3}\,j$ | $-2.976190\times10^{-3}\,j$ | $1.190476\times10^{-3}\,j$ | $-1.984127\times10^{-4}\,j$ | 0 | 0 | 0 |
| 8 | $9.238926\times10^{-4}$ | $-7.185832\times10^{-4}$ | $3.266287\times10^{-4}$ | $-7.537586\times10^{-5}$ | $5.025057\times10^{-6}$ | $2.955916\times10^{-7}$ | $4.667236\times10^{-8}$ |
| 9 | $-1.929012\times10^{-4}\,j$ | $1.533210\times10^{-4}\,j$ | $-7.716049\times10^{-5}\,j$ | $2.204586\times10^{-5}\,j$ | $-2.755732\times10^{-6}\,j$ | 0 | 0 |

We can compare the result of (32) with the result of a numerical integration of $B(x, 2n)$, using (9) and the approximations (11) and (12). If $d_B(n) = 30$, the relative difference is less than $10^{-11}$ for $f \leqslant f_{\max}$ and any value of $n$. If $d_B(n) = 15$, the relative difference is less than $0.2\%$ for $f \leqslant f_{\max}$ and any value of $n$. If $d_B(n) = 5$, the relative difference exceeds $1\%$ above $f_{\max}/4$ for $n = 2$, and exceeds $10\%$ above $f_{\max}/2$ for $n = 1$ and $n = 2$.

### B. EXACT VALUES OF THE WU-KING FACTORS

Some manipulations using (3)–(7) and (29) lead us to the exact values of the Wu-King factors shown in (33)–(35) at the bottom of this page.

The Wu-King factors being dimensionless, we can use (16) to assert that: $A_0$ corresponds to an impedance $z_0 = j\pi\eta A_0$; if $n \in \mathbb{N}$ is nonzero, then $A_n$ corresponds to an impedance $z_n = j\pi\eta A_n/2$; and these impedances satisfy

$$Y_\delta \simeq \sum_{n=0}^{N} \frac{1}{z_n} \,. \tag{36}$$

In other words, $Y_\delta$ is approximately the admittance obtained by connecting $z_0, \ldots, z_N$ in parallel.

It follows from (30)–(31) and (33)–(35) that:

- for any $n \in \mathbb{N}$ and any nonzero $q \in \mathbb{N}$, the coefficient of the term of $A_n$ of degree $q$ in $ka$ is real if $q$ is odd, or imaginary if $q$ is even;
- for any $n \in \mathbb{N}$ and $q \geqslant 2$, the coefficient of the term of $A_n$ of degree $q$ in $ka$ is independent of the frequency and of the characteristics of the antenna;
- at low frequencies, $z_0$ approximately corresponds to an inductive impedance exactly equal to $j\pi\eta$ times the term of $A_0$ of degree 1 in $ka$, so that $z_0 \simeq j\omega L_0$ in which $\omega$ is the radian frequency and the inductance

$$L_0 = \mu a \left[ \mathrm{K}_0\left(\frac{d_w}{2a}\right) \mathrm{I}_0\left(\frac{d_w}{2a}\right) + C_1 \right] \tag{37}$$

  is frequency independent (we use $\mu$ to denote the permeability of the medium);
- the coefficient of the term of $A_0$ of degree 2 in $ka$ is 0 because $\chi_{1\,1} = 0$;
- $\chi_{3\,1} = -j/6$ entails that, at low frequencies, $\mathrm{Re}(z_0)$ approximately corresponds to a frequency-dependent resistance

$$R_r = \eta \frac{\pi}{6}(ka)^4 = \eta \frac{8\pi^5}{3}\left(\frac{a}{\lambda}\right)^4 \,, \tag{38}$$

  which is the approximate radiation resistance of the loop at frequencies where it is electrically small [2, Sec. 2.5], [18, Sec. 6-8];
- for any nonzero $n \in \mathbb{N}$, the coefficient of the term of $A_n$ of degree 1 in $1/ka$ is real;
- at low frequencies, for any nonzero $n \in \mathbb{N}$, $z_n$ approximately corresponds to a capacitive impedance equal to $j\pi\eta/2$ times the term of $A_n$ of degree 1 in $1/ka$;
- the coefficient of the term of $A_1$ of degree 2 in $ka$ is $-j/3$, since $\chi_{1\,0} = -j$, $\chi_{1\,2} = 0$ and $\chi_{3\,1} = -j/6$;
- for $n \geqslant 2$, the coefficient of the term of $A_n$ of degree 2 in $ka$ is zero because $\chi_{1\,(n-1)} = 0$, $\chi_{1\,(n+1)} = 0$ and $\chi_{3\,n} = 0$.

$$A_0 = ka\frac{\mathrm{K}_0\left(\frac{d_w}{2a}\right) \mathrm{I}_0\left(\frac{d_w}{2a}\right) + C_1}{\pi} + \sum_{q=2}^{\infty} \chi_{(q-1)\,1}(ka)^q \,, \tag{33}$$

$$A_1 = -\frac{1}{ka}\,\frac{\mathrm{K}_0\left(\frac{d_w}{2a}\right) \mathrm{I}_0\left(\frac{d_w}{2a}\right) + C_1}{\pi} + ka\left[\frac{\mathrm{K}_0\left(\frac{d_w}{a}\right) \mathrm{I}_0\left(\frac{d_w}{a}\right) + \ln\frac{16a}{d_w} + C_2}{2\pi} - \chi_{2\,1}\right] + \sum_{q=2}^{\infty}\left(\frac{\chi_{(q-1)\,0} + \chi_{(q-1)\,2}}{2} - \chi_{(q+1)\,1}\right)(ka)^q \,, \tag{34}$$

and, for $n \geqslant 2$

$$A_n = -\frac{n^2}{ka}\,\frac{\mathrm{K}_0\left(\frac{nd_w}{2a}\right) \mathrm{I}_0\left(\frac{nd_w}{2a}\right) + C_n}{\pi} + ka\left[\frac{\mathrm{K}_0\left(\frac{(n+1)d_w}{2a}\right) \mathrm{I}_0\left(\frac{(n+1)d_w}{2a}\right) + \mathrm{K}_0\left(\frac{(n-1)d_w}{2a}\right) \mathrm{I}_0\left(\frac{(n-1)d_w}{2a}\right) + C_{n+1} + C_{n-1}}{2\pi} - n^2\chi_{2\,n}\right] + \sum_{q=2}^{\infty}\left(\frac{\chi_{(q-1)\,(n-1)} + \chi_{(q-1)\,(n+1)}}{2} - n^2\chi_{(q+1)\,n}\right)(ka)^q \,. \tag{35}$$

For any $n \in \mathbb{N}$, we consider the power series in the variable $ka$, that is present in (33) if $n = 0$, or (34) if $n = 1$, or (35) if $n \geqslant 2$. It has no constant term and starts with a term proportional to $ka$. We can define an approximation of $A_n$ by utilizing the nonnegative integer $d_A(n)$ such that this power series is replaced with the sum of its terms of degree at most $d_A(n)$ if $d_A(n) \geqslant 1$, or is ignored if $d_A(n) = 0$.

### C. ABOUT THE MODIFIED BESSEL FUNCTIONS

In what follows, we will use Landau's little-o and big-O notations [19, Sec. 5.1]. By [9, Eq. 9.6.12] and [9, Eq. 9.6.13], for any $z \in \mathbb{C}$, we have

$$\mathrm{I}_0(z) = 1 + \frac{z^2}{4} + \frac{z^4}{64} + O(z^6) \tag{39}$$

as $z \to 0$, and

$$\mathrm{K}_0(z) = -\left\{\ln\frac{z}{2} + \gamma\right\}\mathrm{I}_0(z) + \frac{z^2}{4} + \frac{3z^4}{128} + O(z^6) \tag{40}$$

as $z \to 0$. It follows from (39) and (40) that

$$\mathrm{K}_0(z) = -\left(\ln\frac{z}{2} + \gamma\right)\left(1 + \frac{z^2}{4} + \frac{z^4}{64}\right) + \frac{z^2}{4} + \frac{3z^4}{128} + o(z^5)\,. \tag{41}$$

Using (39) and (41), we obtain

$$\mathrm{K}_0(z)\mathrm{I}_0(z) = -\left(\ln\frac{z}{2} + \gamma\right)\left(1 + \frac{z^2}{2} + \frac{3z^4}{32}\right) + \frac{z^2}{4} + \frac{11z^4}{128} + o(z^5)\,, \tag{42}$$

$$\mathrm{K}_0(z)\mathrm{I}_0(z) = -\left(\ln\frac{z}{2} + \gamma\right)\left(1 + \frac{z^2}{2}\right) + \frac{z^2}{4} + o(z^3) \tag{43}$$

and

$$\mathrm{K}_0(z)\mathrm{I}_0(z) = -\ln\frac{z}{2} - \gamma + o(z)\,. \tag{44}$$

We have assumed that $d_w \ll 2a$, so that we can in principle use (42), or (43), or (44) as approximations to remove the modified Bessel functions from (33)–(35). Note that using the coarsest approximation (44) in (37) leads us to

$$L_0 \simeq \mu a\left(\ln\frac{16\,a}{d_w} - 2\right), \tag{45}$$

which is equal to the thin-wire approximation of the external inductance of the loop [20, Eq. (5-100)].

To make sure that one of these approximations is such that the relative error on $\mathrm{K}_0(nd_w/2a)\mathrm{I}_0(nd_w/2a)$ is less than $0.1\%$ up to $n = 21$, a sufficient condition is:

- $d_w/2a$ is less than 0.029 if we use (42);
- $d_w/2a$ is less than 0.014 if we use (43); and
- $d_w/2a$ is less than 0.002 if we use (44).

As a comparison, $d_w/2a = 0.025$ in the case $a = 280\,\mathrm{mm}$ and $d_w = 14\,\mathrm{mm}$ considered above in Section II.D. Thus, a good accuracy could be obtained in this case if we remove the modified Bessel functions from (33)–(35) using (42).

Approximations of $A_0$, $A_1$ and $A_2$ were proposed (without explanations) and discussed in [21, Eq. (71a)–(71c)]. They are based on the use of $d_A(n) = 6$ for $n \in \{0, 1, 2\}$, and on the use of (44) in (33)–(35) to remove the modified Bessel functions.

A word of caution is in order here, about formulas without modified Bessel functions for the computations of what looks like the Wu-King factors, proposed in [22, Eq. (12)–(13)] and [23, Eq. (5-31)–(5-32)]. Though none of these references mention this, these formulas stem from [24, Appendix III] and should not be used today, because they relate to the theory proposed by Storer in [24], which was a significant contribution when it was published, but became obsolete after the theory disclosed by Wu in [3].

## IV. EMISSION

### A. GENERAL RESULTS

We now use a right-handed cartesian coordinate system $(x, y, z)$ arranged according to Fig. 1, and the associated spherical coordinates system $(r, \theta, \varphi)$. We use $(\mathbf{u}_x, \mathbf{u}_y, \mathbf{u}_z)$ to denote the basis of the cartesian coordinate system, and $(\mathbf{u}_r, \mathbf{u}_\theta, \mathbf{u}_\varphi)$ to denote the local orthonormal basis of the spherical coordinate system.

To compute the electric field $\mathbf{E}$ and the magnetic field $\mathbf{H}$ emitted by the loop antenna, we sum the contributions of infinitesimal current elements, regarded as electric dipoles. Using the classical results [25, Sec. 8.5] or [26, Sec. 15.5.5], we obtain

$$\mathbf{E} = \frac{a}{4\pi\epsilon}\int_0^{2\pi}\left\{\left(\frac{1}{R^3} + \frac{jk}{R^2}\right)[3\mathbf{R}_0(\mathbf{R}_0\cdot\mathbf{u}_t) - \mathbf{u}_t] - \frac{k^2}{R}\,\mathbf{R}_0\times(\mathbf{R}_0\times\mathbf{u}_t)\right\}\frac{i_E(\psi)e^{-jkR}}{j\omega}d\psi \tag{46}$$

and

$$\mathbf{H} = \frac{a}{4\pi}\int_0^{2\pi}\left(\frac{1}{R^2} + \frac{jk}{R}\right)\mathbf{u}_t\times\mathbf{R}_0\,i_E(\psi)e^{-jkR}d\psi \tag{47}$$

where $R$ is the distance between the point of spherical coordinates $(a, \pi/2, \psi)$ and the observer, $\mathbf{R}_0$ is a unit vector directed from this point towards the observer, $\mathbf{u}_t$ is a unit vector tangent to the loop wire, its direction being the direction of positive current (which is the direction of increasing $\psi$), and $\epsilon$ is the permittivity of the medium.

Using a numerical integration in (46)–(47), the fields $\mathbf{E}$ and $\mathbf{H}$ can be computed anywhere (though the result will not be accurate very close to the antenna wire, because of the thin wire approximation).

It is interesting to compute $\mathbf{H}$ on the axis of the loop, that is the straight line of equations $x = 0$ and $y = 0$. If the cartesian coordinates of the observer are $(0, 0, z)$, we can use the results of Appendix A to get

$$\mathbf{u}_t\times\mathbf{R}_0 = \frac{z\cos\psi\,\mathbf{u}_x + z\sin\psi\,\mathbf{u}_y + a\mathbf{u}_z}{R}\,, \tag{48}$$

where $R = \sqrt{a^2 + z^2}$. By (20), (47) and (48), $\mathbf{H}$ on the axis of the loop is given by (49) shown at the top of next page.

$$\mathbf{H} \simeq I_0 \frac{a}{4\pi} e^{-jkR} \left( \frac{1}{R^2} + \frac{jk}{R} \right) \int_0^{2\pi} \frac{z\cos\psi \mathbf{u}_x + z\sin\psi \mathbf{u}_y + a\mathbf{u}_z}{R} \frac{\dfrac{1}{A_0} + 2\sum\limits_{n=1}^{N} \dfrac{\cos n\psi}{A_n}}{\dfrac{1}{A_0} + 2\sum\limits_{n=1}^{N} \dfrac{1}{A_n} - \pi\eta\omega C_T} d\psi. \tag{49}$$

Using manipulations involving integrals of $\cos\psi\cos n\psi$ and $\sin\psi\cos n\psi$ over the interval $[0, 2\pi]$, we obtain

$$\mathbf{H} \simeq I_0 \frac{a}{2R^2} e^{-jkR} \frac{\left(\dfrac{1}{R} + jk\right)\left(\dfrac{a\mathbf{u}_z}{A_0} + \dfrac{z\mathbf{u}_x}{A_1}\right)}{\dfrac{1}{A_0} + 2\sum\limits_{n=1}^{N} \dfrac{1}{A_n} - \pi\eta\omega C_T} \tag{50}$$

on the loop axis. At a frequency low enough to be such that $kR \ll 1$, and $1/|A_0| \gg \pi\eta\omega C_T$, and $1/|A_0| \gg 2/|A_n|$ for $n \geqslant 1$, and $a/|A_0| \gg |z|/|A_1|$, we find that (50) leads us to

$$\mathbf{H} \simeq I_0 \frac{a^2}{2R^3} \mathbf{u}_z \,, \tag{51}$$

which is identical to a textbook result on the magnetic field on the axis of a circular loop carrying a dc current [27, Sec. 6-3]. In contrast, if $|z| \gg a$ and the frequency is high enough to be such that $kR \gg 1$ and $a/|A_0| \ll |z|/|A_1|$, we get

$$\mathbf{H} \simeq I_0 \frac{jka}{2RA_1} e^{-jkR} \frac{\pm\,\mathbf{u}_x}{\dfrac{1}{A_0} + 2\sum\limits_{n=1}^{N} \dfrac{1}{A_n} - \pi\eta\omega C_T} \tag{52}$$

on the loop axis, where the plus sign applies to $z > 0$ and the minus sign to $z < 0$. In (52), $||\mathbf{H}||$ varies as $1/R$.

### B. EMISSION IN THE FAR FIELD

We now want to assess $\mathbf{E}$ and $\mathbf{H}$ given by (46)–(47) seen by an observer at the point of spherical coordinates $(r, \theta, \varphi)$, in the case where $r \gg a$ and $kr \gg 1$. According to Appendix A, we have $\mathbf{R}_0 \simeq \mathbf{u}_r$,

$$\mathbf{u}_t \times \mathbf{R}_0 \simeq \cos(\varphi - \psi)\,\mathbf{u}_\theta - \cos\theta \sin(\varphi - \psi)\,\mathbf{u}_\varphi \,, \tag{53}$$

$$-\mathbf{R}_0 \times (\mathbf{R}_0 \times \mathbf{u}_t) \simeq \cos\theta \sin(\varphi - \psi)\,\mathbf{u}_\theta + \cos(\varphi - \psi)\,\mathbf{u}_\varphi \,, \tag{54}$$

and

$$R \simeq r - a\sin\theta\cos(\varphi - \psi) \,. \tag{55}$$

By (20), (46)–(47) and (53)–(55), $\mathbf{E}$ and $\mathbf{H}$ in the far field are given by (56)–(57) shown at the bottom of this page.

For any nonnegative integer $n$, we have

$$\cos(\varphi - \psi)\cos n\psi = \frac{\cos n\varphi}{2}\{\cos[(n+1)\xi] + \cos[(n-1)\xi]\} + \frac{\sin n\varphi}{2}\{\sin[(n+1)\xi] + \sin[(n-1)\xi]\}, \tag{58}$$

where $\xi = \varphi - \psi$. It follows that

$$\begin{aligned} &\int_0^{2\pi} \cos(\varphi - \psi)\cos(n\psi)\, e^{jka\sin\theta\cos(\varphi-\psi)} d\psi \\ &= j^{n+1}\pi\cos(n\varphi)\,[\mathrm{J}_{n+1}(ka\sin\theta) - \mathrm{J}_{n-1}(ka\sin\theta)] \\ &= -j^{n+1}2\pi\cos(n\varphi)\,\mathrm{J}'_n(ka\sin\theta) \,, \end{aligned} \tag{59}$$

in which we have used [9, Eq. 9.1.21] and [9, Eq. 9.1.27]. For any nonnegative integer $n$, we also have

$$\sin(\varphi - \psi)\cos n\psi = \frac{\cos n\varphi}{2}\{\sin[(n+1)\xi] - \sin[(n-1)\xi]\} - \frac{\sin n\varphi}{2}\{\cos[(n+1)\xi] - \cos[(n-1)\xi]\}, \tag{60}$$

where $\xi = \varphi - \psi$. It follows that, in the case where $\theta \neq 0$ and $\theta \neq \pi$, we can again use [9, Eq. 9.1.21] and [9, Eq. 9.1.27] to obtain

$$\begin{aligned} &\int_0^{2\pi} \sin(\varphi - \psi)\cos(n\psi)\, e^{jka\sin\theta\cos(\varphi-\psi)} d\psi \\ &= -j^{n+1}\pi\sin(n\varphi)\,[\mathrm{J}_{n+1}(ka\sin\theta) + \mathrm{J}_{n-1}(ka\sin\theta)] \\ &= -j^{n+1}\frac{2n\pi}{ka\sin\theta}\sin(n\varphi)\,\mathrm{J}_n(ka\sin\theta) \,, \end{aligned} \tag{61}$$

$$\mathbf{E} \simeq I_0 \frac{ak^2}{4\pi\epsilon r} \frac{e^{-jkr}}{j\omega} \int_0^{2\pi} [\cos\theta\sin(\varphi - \psi)\,\mathbf{u}_\theta + \cos(\varphi - \psi)\,\mathbf{u}_\varphi] \frac{\dfrac{1}{A_0} + 2\sum\limits_{n=1}^{N} \dfrac{\cos n\psi}{A_n}}{\dfrac{1}{A_0} + 2\sum\limits_{n=1}^{N} \dfrac{1}{A_n} - \pi\eta\omega C_T} e^{jka\sin\theta\cos(\varphi-\psi)} d\psi \tag{56}$$

and

$$\mathbf{H} \simeq I_0 \frac{jka}{4\pi r} e^{-jkr} \int_0^{2\pi} [\cos(\varphi - \psi)\,\mathbf{u}_\theta - \cos\theta\sin(\varphi - \psi)\,\mathbf{u}_\varphi] \frac{\dfrac{1}{A_0} + 2\sum\limits_{n=1}^{N} \dfrac{\cos n\psi}{A_n}}{\dfrac{1}{A_0} + 2\sum\limits_{n=1}^{N} \dfrac{1}{A_n} - \pi\eta\omega C_T} e^{jka\sin\theta\cos(\varphi-\psi)} d\psi \tag{57}$$

whereas, in the case $\theta = 0$ or $\theta = \pi$, we get

$$\int_0^{2\pi} \sin(\varphi - \psi)\cos(n\psi)\, e^{jka\sin\theta\cos(\varphi-\psi)} d\psi = \begin{cases} \pi \sin\varphi & \text{if } n = 1 \\ 0 & \text{else}. \end{cases} \quad (62)$$

Using (56)–(57), (59) and (61)–(62), we find that: if $\theta \neq 0$ and $\theta \neq \pi$, then $\mathbf{E}$ and $\mathbf{H}$ in the far field are given by (63)–(64) shown at the bottom of this page; whereas, if $\theta = 0$ or $\theta = \pi$, then $\mathbf{E}$ and $\mathbf{H}$ in the far field are given by

$$\mathbf{E} \simeq -I_0\eta \frac{jka}{2rA_1} e^{-jkr} \frac{\cos\theta\sin\varphi\,\mathbf{u}_\theta + \cos\varphi\,\mathbf{u}_\varphi}{\dfrac{1}{A_0} + 2\sum\limits_{n=1}^{N}\dfrac{1}{A_n} - \pi\eta\omega C_T} \quad (65)$$

and

$$\mathbf{H} \simeq I_0 \frac{jka}{2rA_1} e^{-jkr} \frac{\cos\varphi\,\mathbf{u}_\theta - \cos\theta\sin\varphi\,\mathbf{u}_\varphi}{\dfrac{1}{A_0} + 2\sum\limits_{n=1}^{N}\dfrac{1}{A_n} - \pi\eta\omega C_T}, \quad (66)$$

where we have used the fact that, by (25), for any nonnegative integer $n$, the only nonzero $\mathrm{J}_n'(0)$ is $\mathrm{J}_1'(0) = 1/2$. We may use the last results of Appendix A to see that, on the axis of the loop, where $\theta = 0$ or $\theta = \pi$, (66) agrees with (52).

The fields given by (63)–(66) of course satisfy

$$\mathbf{H} \simeq \frac{1}{\eta}\mathbf{u}_r \times \mathbf{E}, \quad (67)$$

since, locally, the fields look like a plane wave propagating in the direction of $\mathbf{u}_r$.

We can express $\mathbf{E}$ in the form $\mathbf{E} = E_r\mathbf{u}_r + E_\theta\mathbf{u}_\theta + E_\varphi\mathbf{u}_\varphi$. Using (13)–(14) and (19) in (63), we obtain, in the far field and in the case where $\theta \neq 0$ and $\theta \neq \pi$,

$$E_r \simeq 0, \quad (68)$$

$$E_\theta \simeq -\frac{\eta\cot\theta}{2r} e^{-jkr} \times \sum_{n=1}^{N} n j^n I_{E\,n} \sin(n\varphi)\mathrm{J}_n(ka\sin\theta) \quad (69)$$

and

$$E_\varphi \simeq -\frac{\eta ka}{2r} e^{-jkr} \times \sum_{n=0}^{N} j^n I_{E\,n} \cos(n\varphi)\mathrm{J}_n'(ka\sin\theta). \quad (70)$$

### C. NOTES ON RELATED WORKS

In 1996, Werner proposed formulas that give the fields emitted by a thin circular loop antenna [28]–[29], for any assumed current distribution specified using the angular Fourier cosine series (1). These impressive but cumbersome formulas use spherical coordinates and are valid everywhere around the antenna. Unlike (46)–(47), they contain no integral. Werner's results for the far-field approximation [28, Eq. (111)–(116)] are consistent with (68)–(70), though they were obtained differently.

In 1997, other formulas for the fields radiated by a thin circular loop antenna were proposed by Li *et al* [30], but they are not advantageous [31]–[32] and use the obsolete concept of dyadic. In 2005, other formulas for the fields radiated by a thin circular loop antenna, based on the use of cylindrical coordinates, were proposed by Conway [33]. Later, other formulas for the fields radiated by a thin circular loop antenna were proposed by Hamed [34]–[36] and Miljak [37].

In 2018, Werner proposed formulas that give the fields emitted by a thin elliptical loop antenna in the far zone [38]. They can be used to assess the effects of an ellipticity of a nominally circular loop antenna.

### D. VECTOR EFFECTIVE LENGTH

Let $\mathbf{h}_E$ be the vector effective length of the loop antenna in a direction $(\theta, \varphi)$, as defined in [2, Sec. 5.2] and [26, Sec. 16.5]. This definition is about emission (a different definition, relating to reception, also exists [39, Sec. 2.15]). According to this definition, in the direction $(\theta, \varphi)$, the vector effective length $\mathbf{h}_E$ is such that $\mathbf{E}$ satisfies

$$\lim_{r\to\infty} r\mathbf{E} = j\eta\frac{I_0\, k\, e^{-jkr}}{4\pi}\mathbf{h}_E. \quad (71)$$

We can express $\mathbf{h}_E$ in the form $\mathbf{h}_E = h_{E\theta}\mathbf{u}_\theta + h_{E\varphi}\mathbf{u}_\varphi$.

$$\mathbf{E} \simeq -I_0\eta\frac{e^{-jkr}}{r} \frac{\cot\theta\left[\sum\limits_{n=1}^{N}\dfrac{nj^n\sin(n\varphi)\,\mathrm{J}_n(ka\sin\theta)}{A_n}\right]\mathbf{u}_\theta + ka\left[\dfrac{\mathrm{J}_0'(ka\sin\theta)}{2A_0} + \sum\limits_{n=1}^{N}\dfrac{j^n\cos(n\varphi)\,\mathrm{J}_n'(ka\sin\theta)}{A_n}\right]\mathbf{u}_\varphi}{\dfrac{1}{A_0} + 2\sum\limits_{n=1}^{N}\dfrac{1}{A_n} - \pi\eta\omega C_T} \quad (63)$$

and

$$\mathbf{H} \simeq I_0\frac{e^{-jkr}}{r} \frac{ka\left[\dfrac{\mathrm{J}_0'(ka\sin\theta)}{2A_0} + \sum\limits_{n=1}^{N}\dfrac{j^n\cos(n\varphi)\,\mathrm{J}_n'(ka\sin\theta)}{A_n}\right]\mathbf{u}_\theta - \cot\theta\left[\sum\limits_{n=1}^{N}\dfrac{nj^n\sin(n\varphi)\,\mathrm{J}_n(ka\sin\theta)}{A_n}\right]\mathbf{u}_\varphi}{\dfrac{1}{A_0} + 2\sum\limits_{n=1}^{N}\dfrac{1}{A_n} - \pi\eta\omega C_T} \quad (64)$$

According to (63) and (65), we obtain:

$$h_{E\theta} \simeq 4j\pi \frac{\cot\theta}{k} \frac{\sum_{n=1}^{N} \frac{nj^n \sin(n\varphi)\, \mathrm{J}_n(ka\sin\theta)}{A_n}}{\frac{1}{A_0} + 2\sum_{n=1}^{N} \frac{1}{A_n} - \pi\eta\omega C_T} \tag{72}$$

in the case where $\theta \neq 0$ and $\theta \neq \pi$;

$$h_{E\theta} \simeq -\frac{2\pi a}{A_1} \frac{\cos\theta \sin\varphi}{\frac{1}{A_0} + 2\sum_{n=1}^{N} \frac{1}{A_n} - \pi\eta\omega C_T} \tag{73}$$

in the case where $\theta = 0$ or $\theta = \pi$; and

$$h_{E\varphi} \simeq 2j\pi a \frac{\frac{\mathrm{J}_0'(ka\sin\theta)}{A_0} + 2\sum_{n=1}^{N} \frac{j^n \cos(n\varphi)\, \mathrm{J}_n'(ka\sin\theta)}{A_n}}{\frac{1}{A_0} + 2\sum_{n=1}^{N} \frac{1}{A_n} - \pi\eta\omega C_T}. \tag{74}$$

We observe that, if $\theta = \pi/2$, or if $\varphi = 0$ or $\varphi = \pi$, then $h_{E\theta} = 0$. Let $\varphi_X \in [0, 2\pi)$. Since, for any nonnegative integer $n$, the only nonzero $\mathrm{J}_n'(0)$ is $\mathrm{J}_1'(0) = 1/2$, we observe that, if $\theta = 0$ or $\theta = \pi$, then the value of $|h_{E\varphi}|$ for $\varphi = \varphi_X$ is equal to the value of $|h_{E\theta}|$ for $\varphi = \varphi_X + \pi/2$.

At a frequency where the loop is electrically small, we can use expansions of $h_{E\theta}$ and $h_{E\varphi}$ for small values of $ka$. It follows from (25) that, for small values of $x$,

$$\mathrm{J}_n(x) = \frac{1}{n!}\left(\frac{x}{2}\right)^n \left(1 - \frac{x^2}{4(n+1)} + o(x^3)\right), \tag{75}$$

$$\mathrm{J}_0'(x) = -\frac{x}{2} + \frac{x^3}{16} + o(x^4) \tag{76}$$

and

$$\mathrm{J}_n'(x) = \frac{1}{2\,n!}\left(\frac{x}{2}\right)^{n-1} \left(n - \frac{(n+2)x^2}{4(n+1)} + o(x^3)\right), \tag{77}$$

where $n$ is a positive integer. To get the wanted expansions, we must also take into account the fact that, according to Fig. 4 and (33)–(35), for $ka \to 0$, we have $1/A_0 = O(1/ka)$, and $1/A_n = O(ka)$ if $n$ is positive. Thus, for small values of $ka$, it follows from (72)–(74) that $h_{E\theta}$ and $h_{E\varphi}$ are approximately given by (78)–(79) shown at the bottom of the page, where $w = ka\sin\theta$. These formula are new.

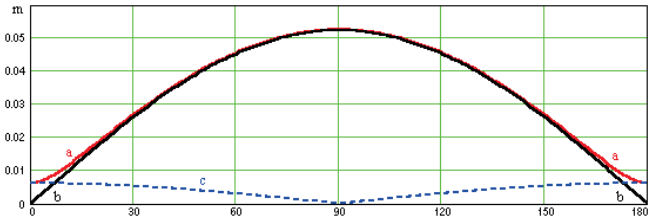


**FIGURE 9.** Entries of the vector effective length at about 10.0 MHz, as a function of $\theta$ in degrees: $|h_{E\varphi}|$ for $\varphi = \pi$ is curve "a"; $|h_{E\varphi}|$ for $\varphi = \pi/2$ is curve "b"; $|h_{E\theta}|$ for $\varphi = \pi/2$ is curve "c"; and $|h_{E\theta}|$ for $\varphi = 0$ or $\varphi = \pi$ is not shown but equal to 0.

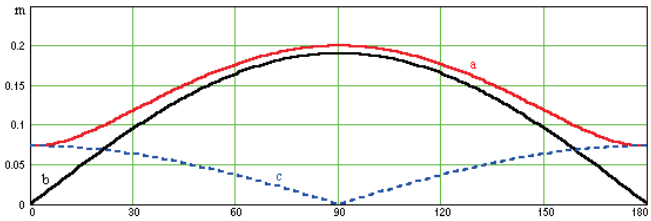


**FIGURE 10.** Entries of the vector effective length at about 31.6 MHz, as a function of $\theta$ in degrees: $|h_{E\varphi}|$ for $\varphi = \pi$ is curve "a"; $|h_{E\varphi}|$ for $\varphi = \pi/2$ is curve "b"; $|h_{E\theta}|$ for $\varphi = \pi/2$ is curve "c"; and $|h_{E\theta}|$ for $\varphi = 0$ or $\varphi = \pi$ is not shown but equal to 0.

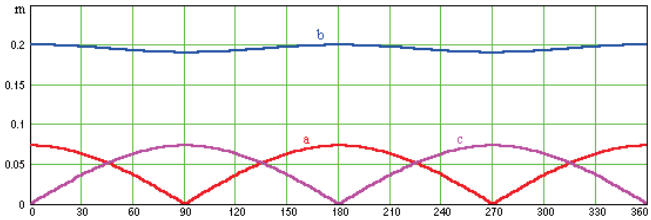


**FIGURE 11.** Entries of the vector effective length at about 31.6 MHz, as a function of $\varphi$ in degrees: $|h_{E\varphi}|$ for $\theta = 0$ is curve "a"; $|h_{E\varphi}|$ for $\theta = \pi/2$ is curve "b"; $|h_{E\theta}|$ for $\theta = 0$ is curve "c"; and $|h_{E\theta}|$ for $\theta = \pi/2$ is not shown but equal to 0.

Less accurately, we also have

$$\mathbf{h}_E \simeq -j\pi k a^2 \sin\theta\, \mathbf{u}_\varphi + o(ka). \tag{80}$$

### E. EXAMPLES

We use again the case where $a = 280\,\mathrm{mm}$ and $d_w = 14\,\mathrm{mm}$ defined in Section II.D, for which $d_w/2a = 0.025$.

Fig. 9 to Fig. 14 show $|h_{E\theta}|$ and $|h_{E\varphi}|$ given by (72)–(74), as a function of $\theta$ and $\varphi$, at about 10.0 MHz, 31.6 MHz, 79.4 MHz (near the first parallel resonance, at $ka \simeq 0.47$),

$$h_{E\theta} \simeq 2j\pi a\cos\theta \frac{j\frac{\sin\varphi}{A_1}\left(1 - \frac{w^2}{8}\right) - \frac{\sin 2\varphi}{2A_2}w - j\frac{\sin 3\varphi}{8A_3}w^2 + o((ka)^3)}{\frac{1}{A_0} + 2\sum_{n=1}^{N}\frac{1}{A_n} - \pi\eta\omega C_T} \tag{78}$$

and

$$h_{E\varphi} \simeq 2j\pi a \frac{-\frac{1}{2A_0}w\left(1 - \frac{w^2}{8}\right) + j\frac{\cos\varphi}{A_1}\left(1 - \frac{3w^2}{8}\right) - \frac{\cos 2\varphi}{2A_2}w - j\frac{\cos 3\varphi}{8A_3}w^2 + o((ka)^3)}{\frac{1}{A_0} + 2\sum_{n=1}^{N}\frac{1}{A_n} - \pi\eta\omega C_T}. \tag{79}$$

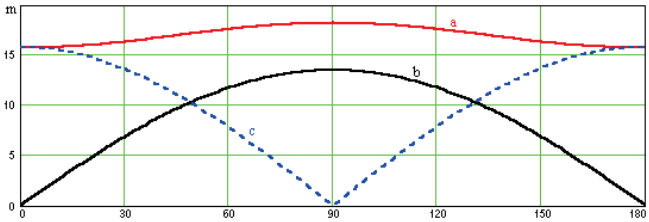


**FIGURE 12.** Entries of the vector effective length at about 79.4 MHz, as a function of $\theta$ in degrees: $|h_{E\varphi}|$ for $\varphi = \pi$ is curve "a"; $|h_{E\varphi}|$ for $\varphi = \pi/2$ is curve "b"; $|h_{E\theta}|$ for $\varphi = \pi/2$ is curve "c"; and $|h_{E\theta}|$ for $\varphi = 0$ or $\varphi = \pi$ is not shown but equal to 0.

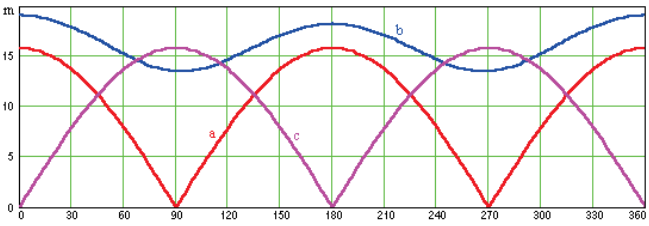


**FIGURE 13.** Entries of the vector effective length at about 79.4 MHz, as a function of $\varphi$ in degrees: $|h_{E\varphi}|$ for $\theta = 0$ is curve "a"; $|h_{E\varphi}|$ for $\theta = \pi/2$ is curve "b"; $|h_{E\theta}|$ for $\theta = 0$ is curve "c"; and $|h_{E\theta}|$ for $\theta = \pi/2$ is not shown but equal to 0.

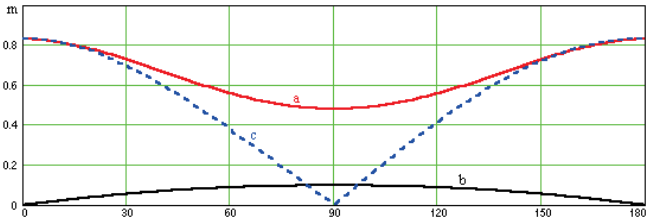


**FIGURE 14.** Entries of the vector effective length at about 178 MHz, as a function of $\theta$ in degrees: $|h_{E\varphi}|$ for $\varphi = \pi$ is curve "a"; $|h_{E\varphi}|$ for $\varphi = \pi/2$ is curve "b"; $|h_{E\theta}|$ for $\varphi = \pi/2$ is curve "c"; and $|h_{E\theta}|$ for $\varphi = 0$ or $\varphi = \pi$ is not shown but equal to 0.

and 178 MHz (near the first series resonance, at $ka \simeq 1.05$). Fig. 15 shows $|h_{E\theta}|$ and $|h_{E\varphi}|$ given by (72)–(74), as a function of the frequency.

Fig. 16 shows the discrepancies between the accurate formulas (72)–(74) and the approximate formulas (78)–(79), as a function of the frequency. The latter are found to be very accurate up to 200 MHz (for which $ka \simeq 1.17$), well beyond the first parallel resonance and the first series resonance.

Fig. 15 shows that the behavior predicted by (80) is accurate up to about 30 MHz (for which $ka \simeq 0.18$).

### F. GAIN

The gain of the antenna in a specified direction is given by

$$G = \frac{\eta k^2}{4\pi \mathrm{Re}(Z_{ant})}(|h_{E\theta}|^2 + |h_{E\varphi}|^2). \tag{81}$$

At low enough frequencies, we can use (80) and the fact that $\mathrm{Re}(Z_{ant})$ is close to $R_r$ given by (38), to obtain

$$G \simeq \frac{3}{2}\sin^2\theta. \tag{82}$$

Fig. 17 shows $G$ given by (81), as a function of the frequency, for the same loop antenna as the one considered

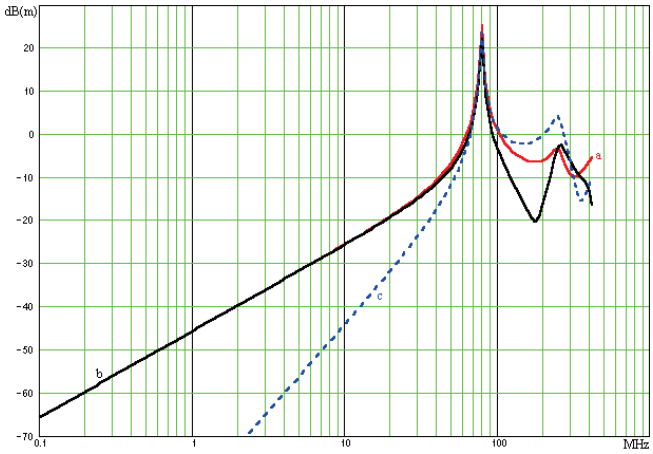


**FIGURE 15.** Entries of the vector effective length, versus frequency. $|h_{E\varphi}|$ for $\theta = \pi/2$ and $\varphi = \pi$ is curve "a". $|h_{E\varphi}|$ for $\theta = \pi/2$ and $\varphi = \pi/2$ is curve "b". $|h_{E\theta}|$ for $\theta = 0$ and $\varphi = \pi/2$ is curve "c".

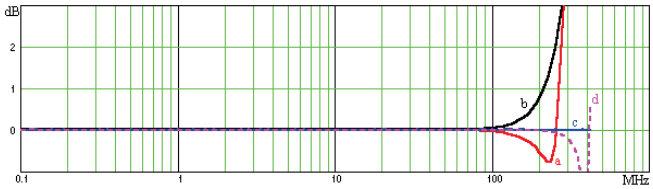


**FIGURE 16.** Deviations of (78)–(79) from (72)–(74): $|h_{E\varphi}|$ for $\theta = \pi/2$ and $\varphi = \pi$ is curve "a"; $|h_{E\varphi}|$ for $\theta = \pi/2$ and $\varphi = \pi/2$ is curve "b"; $|h_{E\theta}|$ for $\theta = 0$ and $\varphi = \pi/2$ is curve "c"; $|h_{E\theta}|$ for $\theta = \pi/4$ and $\varphi = \pi/2$ is curve "d".

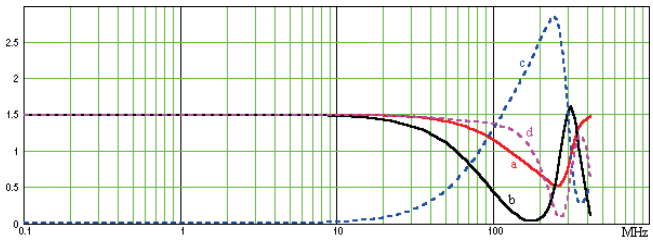


**FIGURE 17.** Gain, versus frequency. $G$ for $\theta = \pi/2$ and $\varphi = \pi$ is curve "a". $G$ for $\theta = \pi/2$ and $\varphi = \pi/2$ is curve "b". $G$ for $\theta = 0$ and $\varphi = \pi/2$ is curve "c". $G$ for $\theta = \pi/2$ and $\varphi = 0$ is curve "d".

in Fig. 9 to Fig. 16. We see that the approximation (82) is accurate up to about 20 MHz (for which $ka \simeq 0.12$). It follows that, up to 20 MHz, the maximum gain occurs for $\theta = \pi/2$ and practically any value of $\varphi$. We have not found the direction of maximum gain at higher frequencies, in the literature [14, Sec. 5-3]. We used a maximum seeking algorithm to ascertain that, for this loop antenna:

- at about 31.6 MHz (for which $ka \simeq 0.19$), the maximum gain is about 1.47, and occurs in the direction $\theta = \pi/2$ and $\varphi = 0$, which is consistent with Fig. 10 and Fig. 11;
- at about 79.4 MHz (near the first parallel resonance), the maximum gain is about 1.40, and occurs in the direction $\theta = \pi/2$ and $\varphi = 0$, which is consistent with Fig. 12 and Fig. 13; and
- at about 178 MHz (near the first series resonance), the maximum gain is about 2.29, and occurs in the directions $\theta = 0$ or $\theta = \pi$, in line with Fig. 14.

## V. RECEPTION

### A. GENERAL RESULTS

This Section V presents new results about the loop antenna used for receiving an arbitrary incident time-harmonic electromagnetic field $\mathcal{F}_i = (\mathbf{E}_i, \mathbf{H}_i)$. The open-circuit voltage at the antenna terminals is denoted by $e_{ant}$. The results presented in [40, Sec. IV-Sec. V] and [41, Sec. IV] seem to be only applicable to a planar wire loop antenna without terminal-zone network. However, they are based on [40, Eq. (1)], that is to say

$$e_{ant} = -\frac{1}{I_0} \iiint_{\text{Antenna}} \mathbf{J}_t \cdot \mathbf{E}_i \, dv \,, \tag{83}$$

where $\mathbf{J}_t$ is the current density in the antenna if it is used for emission and a current $I_0$ flows into the positive terminal of the antenna port, where $\mathbf{E}_i$ is the incident electric field, and where $dv$ is a volume element. This formula is based on reciprocity and applicable to any antenna in which no non-reciprocal phenomenon occurs [42, Sec. 13.06]. If we apply this formula to our antenna, we observe that the volume integral over the lumped capacitance $C_T$ and the lumped inductance $L_T$ can be ignored because a lumped capacitance or inductance has no physical size, and our model assumes that the only effective current in the antenna wire is the current distribution $i_E(\psi)$.

It follows that we can directly apply the results presented in [40, Sec. IV-Sec. V] and [41, Sec. IV] to the loop antenna considered in this article, which includes a terminal-zone network. Thus, using [40, Eq. (73)] or [41, Eq. (75)], we obtain

$$e_{ant} = j\omega\mu \iint_{\mathcal{A}} \mathbf{H}_i \cdot \mathbf{u}_z \, d\mathcal{A} - a \int_0^{2\pi} \frac{i_E(\psi) - I_0}{I_0} \, \mathbf{u}_t \cdot \mathbf{E}_i \, d\psi \,, \tag{84}$$

where $\mathcal{A}$ denotes the disk bounded by the center line of the loop antenna, $d\mathcal{A}$ is a surface element of $\mathcal{A}$, and $\mathbf{u}_t$ was defined in Section IV.A. This formula is equivalent to

$$e_{ant} = -a \int_0^{2\pi} \frac{i_E(\psi)}{I_0} \, \mathbf{u}_t \cdot \mathbf{E}_i \, d\psi \,. \tag{85}$$

An alternative proof of (84)–(85) is shown in Appendix B.

If we decompose $\mathcal{F}_i = (\mathbf{E}_i, \mathbf{H}_i)$ into the 4 elementary time-harmonic electromagnetic fields (ETHEFs) defined in [40]–[41], denoted by $\mathcal{F}_A = (\mathbf{E}_A, \mathbf{H}_A)$, $\mathcal{F}_B = (\mathbf{E}_B, \mathbf{H}_B)$, $\mathcal{F}_C = (\mathbf{E}_C, \mathbf{H}_C)$ and $\mathcal{F}_D = (\mathbf{E}_D, \mathbf{H}_D)$, it follows from (84) that we can also use [40, Eq. (71)] or [41, Eq. (73)], that is to say

$$e_{ant} = j\omega\mu \iint_{\mathcal{A}} \mathbf{H}_A \cdot \mathbf{u}_z \, d\mathcal{A} - a \int_0^{2\pi} \frac{i_E(\psi) - I_0}{I_0} \, \mathbf{u}_t \cdot (\mathbf{E}_A + \mathbf{E}_B) \, d\psi \,. \tag{86}$$

Thus, at any frequency, only $\mathcal{F}_A$ and $\mathcal{F}_B$ excite the loop antenna. Moreover, in the context of low-frequency field measurements, it is possible to consider that $\mathcal{F}_A$ causes the intended response of the antenna, while $\mathcal{F}_B$ may cause an unwanted response. What follows will allow us to clarify the meaning of "the context of low-frequency field measurements" in the previous sentence.

### B. RECEPTION OF UNIFORM PLANE WAVES

We now assume that $\mathcal{F}_i$ is a uniform time-harmonic plane wave propagating from the direction $\theta = \theta_i$ and $\varphi = \varphi_i$. The wave vector of this incident plane wave is

$$\mathbf{k}_i = -k \sin\theta_i (\cos\varphi_i \mathbf{u}_x + \sin\varphi_i \mathbf{u}_y) - k \cos\theta_i \mathbf{u}_z \,. \tag{87}$$

Let $\mathbf{E}_{i0}$ be $\mathbf{E}_i$ at the origin. We use $(\mathbf{u}_{ri}, \mathbf{u}_{\theta i}, \mathbf{u}_{\varphi i})$ to denote the local orthonormal basis of the spherical coordinate system in the direction $\theta = \theta_i$ and $\varphi = \varphi_i$. Since $\mathbf{E}_{i0} \cdot \mathbf{k}_i = 0$, we can express $\mathbf{E}_{i0}$ in the form $\mathbf{E}_{i0} = E_{i0\theta} \mathbf{u}_{\theta i} + E_{i0\varphi} \mathbf{u}_{\varphi i}$. We have

$$\mathbf{E}_i = \mathbf{E}_{i0} \, e^{-j\mathbf{k}_i \cdot \mathbf{r}} = (E_{i0\theta} \mathbf{u}_{\theta i} + E_{i0\varphi} \mathbf{u}_{\varphi i}) \, e^{-j\mathbf{k}_i \cdot \mathbf{r}} \,, \tag{88}$$

where $\mathbf{r}$ is the radius vector of the observer. If we now assume that the observer is located on the center line of the electric conductor, at the angle $\psi$ shown in Fig. 1, we have

$$\mathbf{k}_i \cdot \mathbf{r} = -ka \sin\theta_i \cos(\varphi_i - \psi) \,. \tag{89}$$

It follows from (113) of Appendix A that

$$\mathbf{u}_t \cdot \mathbf{E}_i = \left[ \cos\theta_i \sin(\varphi_i - \psi) \, E_{i0\theta} + \cos(\varphi_i - \psi) \, E_{i0\varphi} \right] e^{jka \sin\theta_i \cos(\varphi_i - \psi)} \,. \tag{90}$$

Using (90) in (85), and comparing the result with (56), we find that, if $\mathbf{E}$ is the field radiated by the loop antenna in the direction $\theta = \theta_i$ and $\varphi = \varphi_i$ during emission, we get

$$\lim_{r\to\infty} r\mathbf{E} \cdot \mathbf{E}_{i0} = -I_0 \frac{k^2}{4\pi\epsilon} \frac{e^{-jkr}}{j\omega} e_{ant} \,. \tag{91}$$

Using (71) in (91), we obtain

$$e_{ant} = \mathbf{h}_{Ei} \cdot \mathbf{E}_{i0} \,, \tag{92}$$

where $\mathbf{h}_{Ei}$ is the vector effective length of the loop antenna in the direction $\theta = \theta_i$ and $\varphi = \varphi_i$. This result, which only applies to the circumstance in which $\mathcal{F}_i$ is a uniform plane wave, is well known [2, Sec. 5.2], [26, Sec. 16.5], [43, Sec. 4.5]. We have derived it here to show that it is a direct consequence of (84) or (85), which are applicable to an incident $\mathcal{F}_i$ that need not be a uniform plane wave.

According to [40, Appendix D], in the plane $z = 0$, $\mathcal{F}_A$ and $\mathcal{F}_B$ satisfy

$$\mathbf{E}_A = E_{i0\varphi} \, \mathbf{u}_{\varphi i} \, e^{-j\mathbf{k}_i \cdot \mathbf{r}} \,, \tag{93}$$

$$\mathbf{H}_A = -\frac{1}{\eta} \sin\theta_i \, E_{i0\varphi} \, \mathbf{u}_z \, e^{-j\mathbf{k}_i \cdot \mathbf{r}} \tag{94}$$

and

$$\mathbf{E}_B = \cos\theta_i \, E_{i0\theta} \, (\cos\varphi_i \mathbf{u}_x + \sin\varphi_i \mathbf{u}_y) \, e^{-j\mathbf{k}_i \cdot \mathbf{r}} \,, \tag{95}$$

where, in the case $\theta_i = 0$ or $\theta_i = \pi$, the arbitrary $\varphi_i$ is chosen in such a way that $\mathbf{E}_{i0} = E_{i0\varphi} \, \mathbf{u}_{\varphi i}$.

If we express $\mathbf{h}_{Ei}$ in the form $\mathbf{h}_{Ei} = h_{Ei\theta}\mathbf{u}_{\theta i} + h_{Ei\varphi}\mathbf{u}_{\varphi i}$, (92) leads us to

$$e_{ant} = h_{Ei\theta}E_{i0\theta} + h_{Ei\varphi}E_{i0\varphi} \tag{96}$$

where $E_{i0\theta}$ and $E_{i0\varphi}$ are independent arbitrary parameters that define the arbitrary incident uniform plane wave $\mathcal{F}_i$.

Using (93)–(95) in (86), and comparing the result to (96) in a context where $E_{i0\theta}$ and $E_{i0\varphi}$ are regarded as independent and arbitrary, we find that the contribution of $\mathcal{F}_A$ to $e_{ant}$ is $h_{Ei\varphi}E_{i0\varphi}$, and the contribution of $\mathcal{F}_B$ to $e_{ant}$ is $h_{Ei\theta}E_{i0\theta}$. If $e_{ant}$ is computed using (92) and the approximate value of $\mathbf{h}_{Ei}$ given by (80), only $\mathcal{F}_A$ is (coarsely) taken into account.

Since we have already investigated $Z_{ant}$, $h_{Ei\varphi}$ and $h_{Ei\theta}$ as a function of the frequency, it follows from (96) that we have all the ingredients of a Thevenin equivalent circuit of the circular loop antenna used for reception. For a Norton equivalent circuit, we need the short-circuit current of the loop antenna used for reception, which is given by

$$i_{ant} = \frac{\mathbf{h}_{Ei}\cdot\mathbf{E}_{i0}}{Z_{ant}} = \frac{h_{Ei\theta}E_{i0\theta} + h_{Ei\varphi}E_{i0\varphi}}{Z_{ant}}\,. \tag{97}$$

The loop antenna parameters $h_{Ei\theta}/Z_{ant}$ and $h_{Ei\varphi}/Z_{ant}$ are therefore relevant to the Norton equivalent circuit. It follows from (17) and (72)–(74) that, if $L_T = 0$, we obtain:

$$\frac{h_{Ei\theta}}{Z_{ant}} \simeq \frac{4\cot\theta_i}{\eta k}\sum_{n=1}^{N}\frac{nj^n\sin(n\varphi_i)\,\mathrm{J}_n(ka\sin\theta_i)}{A_n} \tag{98}$$

in the case where $\theta_i \neq 0$ and $\theta_i \neq \pi$;

$$\frac{h_{Ei\theta}}{Z_{ant}} \simeq j\frac{2a}{\eta A_1}\cos\theta_i\sin\varphi_i \tag{99}$$

in the case where $\theta_i = 0$ or $\theta_i = \pi$; and

$$\frac{h_{Ei\varphi}}{Z_{ant}} \simeq \frac{2a}{\eta}\left[\frac{\mathrm{J}_0'(ka\sin\theta_i)}{A_0} + 2\sum_{n=1}^{N}\frac{j^n\cos(n\varphi_i)\,\mathrm{J}_n'(ka\sin\theta_i)}{A_n}\right]. \tag{100}$$

For small values of $ka$ and $L_T = 0$, it follows from (78)–(79) that $h_{Ei\theta}/Z_{ant}$ and $h_{Ei\varphi}/Z_{ant}$ are approximately

$$\frac{h_{Ei\theta}}{Z_{ant}} \simeq \frac{2a\cos\theta_i}{\eta}\left[j\frac{\sin\varphi_i}{A_1}\left(1-\frac{w^2}{8}\right) - \frac{\sin 2\varphi_i}{2A_2}w - j\frac{\sin 3\varphi_i}{8A_3}w^2 + o((ka)^3)\right] \tag{101}$$

and

$$\frac{h_{Ei\varphi}}{Z_{ant}} \simeq \frac{2a}{\eta}\left[\frac{-1}{2A_0}w\left(1-\frac{w^2}{8}\right) + j\frac{\cos\varphi_i}{A_1}\left(1-\frac{3w^2}{8}\right) - \frac{\cos 2\varphi_i}{2A_2}w - j\frac{\cos 3\varphi_i}{8A_3}w^2 + o((ka)^3)\right], \tag{102}$$

where $w = ka\sin\theta_i$. Less accurately, we also have

$$\frac{\mathbf{h}_{Ei}}{Z_{ant}} \simeq -\frac{\pi a^2}{cL_0}\sin\theta_i\,\mathbf{u}_{\varphi i} + o(1), \tag{103}$$

in which $L_0$ is the inductance defined by (37).

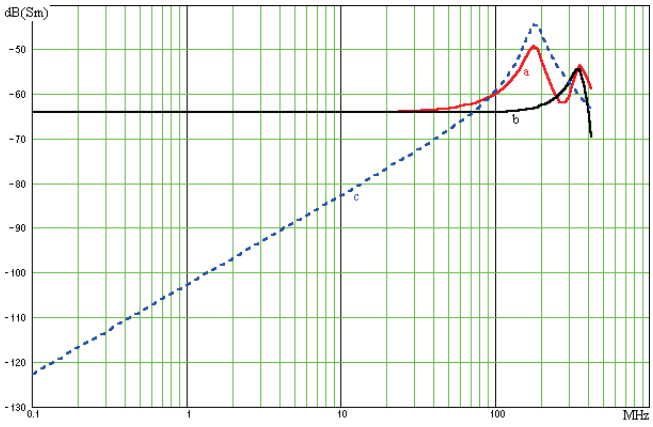


**FIGURE 18.** Components of $\mathbf{h}_{Ei}/Z_{ant}$, as a function of the frequency. $|h_{Ei\varphi}/Z_{ant}|$ for $\theta = \pi/2$ and $\varphi = \pi$ is curve "a". $|h_{Ei\varphi}/Z_{ant}|$ for $\theta = \pi/2$ and $\varphi = \pi/2$ is curve "b". $|h_{Ei\theta}/Z_{ant}|$ for $\theta = 0$ and $\varphi = \pi/2$ is curve "c".

The contribution of $\mathcal{F}_A$ to $i_{ant}$ is $h_{Ei\varphi}E_{i0\varphi}/Z_{ant}$, and the contribution of $\mathcal{F}_B$ to $i_{ant}$ is $h_{Ei\theta}E_{i0\theta}/Z_{ant}$. If $i_{ant}$ is computed using (97) and the approximate value of $\mathbf{h}_{Ei}/Z_{ant}$ given by (103), only $\mathcal{F}_A$ is (coarsely) taken into account.

Fig. 18 shows $|h_{Ei\theta}/Z_{ant}|$ and $|h_{Ei\varphi}/Z_{ant}|$ given by (98)–(100), as a function of the frequency, for the antenna considered in Section IV.E (in which $L_T = 0$).

Expressed in decibels, the deviations between the accurate formulas (98)–(100) and the approximate formulas (101)–(102) are the same as the corresponding deviations between the accurate formulas (72)–(74) and the approximate formulas (78)–(79). Thus, the approximate formulas (101)–(102) are very accurate up to 200 MHz or $ka \simeq 1.17$.

Fig. 18 shows that the behavior predicted by (103) is accurate up to about 30 MHz or $ka \simeq 0.18$.

### C. ABOUT DIRECTION FINDING AND MEASUREMENTS

We have up to now only considered a circular loop antenna in free space, so that we have ignored the effects of nearby ground and/or objects, and of a feeder, on the received signal. A discussion of these phenomena is outside the scope of this article. Our models nevertheless directly provide some clues on direction finding and electromagnetic field measurements using an electrically small circular loop antenna.

In direction finding, the loop antenna is typically rotated until a very small response (ideally, a null response) is obtained from a receiver coupled to the antenna [44, p. 875], [45, Ch. 3], [46, Sec. 1.04], [47, Sec. 39-2]. It is assumed that this very small response indicates that the plane of the loop is perpendicular to the direction in which a received uniform plane wave propagates, that is to say $\theta_i = 0$ or $\theta_i = \pi$. It follows from (78)–(79) or (101)–(102) that a very small response is obtained for any polarization of this incident wave if the frequency is such that $|1/A_1| \ll |ka/A_0|/2$.

In electromagnetic field measurements, a reasonable purpose of the measurement is to obtain information about $\mathcal{F}_A$, in spite of possible unwanted effects of $\mathcal{F}_B$ [40, Sec. X], [41, Sec. VII]. It follows from (78)–(79) or (101)–(102) that this result is achieved by positioning the loop in such a way

that the direction in which a received uniform plane wave propagates satisfies $\theta_i = \pi/2$.

In addition, one may wish that $|i_{ant}/E_{i0\varphi}|$ is substantially frequency independent up to the largest possible frequency. This is particularly relevant to configurations in which the loop antenna is suitably coupled to an amplifier having an input impedance whose absolute value is much less than $|Z_{ant}|$ over a broad frequency range, and having a practically constant transimpedance over this broad frequency range. According to (102), $|i_{ant}/E_{i0\varphi}|$ is substantially frequency independent up to the largest possible frequency by positioning the loop in such a way that $\theta_i = \pi/2$ and $\varphi_i = \pm\pi/2$, and by utilizing a loop such that $|1/A_2| \ll |1/A_0|$. In Fig. 18, this result is obtained up to about 168 MHz, corresponding to $ka \simeq 0.99$ and $2a/\lambda \simeq 0.314$, for a deviation of about 1 dB from the value at 100 kHz.

In contrast, if $\theta_i$ and $\varphi_i$ are unknown, the unwanted effects of $\mathcal{F}_B$ are small if $|1/A_1| \ll |ka/A_0|/2$, according to (78)–(79) or (101)–(102). We find that a difference of at least 20 dB between the curves "b" and "c" of Fig. 15 or Fig. 18 is obtained only up to about 8.4 MHz, which corresponds to $ka \simeq 0.049$ and $2a/\lambda \simeq 0.016$.

This discussion of electromagnetic field measurements supplements the one proposed in [48], where a loop antenna such that $2a/\lambda \leqslant 0.010$ is recommended for measuring unknown magnetic fields.

## VI. CONCLUSION

We have studied a single-turn circular wire loop antenna lying in a homogeneous and lossless medium.

In this endeavor, we used known explicit mathematical models of the current distribution in the loop antenna and the impedance presented by the loop antenna. These models contain no details of the geometry of the terminal region, but include a terminal-zone network that allows the possibility of taking this geometry into account. We obtained improved equivalent formulas and approximate formulas for these models. In particular, (33)–(35) are quite efficient for very accurate computations of the Wu-King factors.

We derived mathematical models for emission by the loop antenna, which include new approximate but accurate formulas for the computation of the vector effective length.

We obtained new mathematical models for reception by the loop antenna, including results involving the elementary time-harmonic electromagnetic fields $\mathcal{F}_A$ and $\mathcal{F}_B$. We also explained how these results can be applied to direction finding and measurements.

A limitation of our work is that we have not taken into account the resistance of the conductor forming the antenna.

This article is relevant to antenna theory and applications where accuracy is important, among which electromagnetic compatibility (EMC), electromagnetic field measurements, antenna calibration, direction finding, etc. A forthcoming article will show how some of the mathematical models presented in this article can be used to obtain circuit models of the circular wire loop antenna, and to design innovative shielded loop antennas.

## APPENDIX A

This appendix provides some details on the derivations of Section IV. Let Q be the point where the observer lies, and P a point on the center line of the solid torus mentioned in Section II.A, at the angle $\psi$ shown in Fig. 1. At this angle, the vector $\mathbf{u}_t$ defined in Section IV.A is

$$\mathbf{u}_t = -\sin\psi\mathbf{u}_x + \cos\psi\mathbf{u}_y\,. \tag{104}$$

In Section IV.A, when we assume that the cartesian coordinates of the observer are $(0, 0, z)$, we have

$$\overrightarrow{\mathrm{PQ}} = -a\cos\psi\mathbf{u}_x - a\sin\psi\mathbf{u}_y + z\mathbf{u}_z\,, \tag{105}$$

so that

$$R = ||\overrightarrow{\mathrm{PQ}}|| = \sqrt{a^2 + z^2} \tag{106}$$

and

$$\mathbf{R}_0 = \frac{\overrightarrow{\mathrm{PQ}}}{||\overrightarrow{\mathrm{PQ}}||} = \frac{-a\cos\psi\mathbf{u}_x - a\sin\psi\mathbf{u}_y + z\mathbf{u}_z}{R}\,. \tag{107}$$

By (104) and (107), $\mathbf{u}_t \times \mathbf{R}_0$ is given by (48).

The observer may now lie anywhere, at the spherical coordinates $(r, \theta, \varphi)$. We have

$$\mathbf{u}_r = \sin\theta\cos\varphi\,\mathbf{u}_x + \sin\theta\sin\varphi\,\mathbf{u}_y + \cos\theta\,\mathbf{u}_z\,, \tag{108}$$

$$\mathbf{u}_\theta = \cos\theta\cos\varphi\,\mathbf{u}_x + \cos\theta\sin\varphi\,\mathbf{u}_y - \sin\theta\,\mathbf{u}_z\,, \tag{109}$$

and

$$\mathbf{u}_\varphi = -\sin\varphi\,\mathbf{u}_x + \cos\varphi\,\mathbf{u}_y\,. \tag{110}$$

It follows that

$$\mathbf{u}_x = \sin\theta\cos\varphi\,\mathbf{u}_r + \cos\theta\cos\varphi\,\mathbf{u}_\theta - \sin\varphi\,\mathbf{u}_\varphi \tag{111}$$

and

$$\mathbf{u}_y = \sin\theta\sin\varphi\,\mathbf{u}_r + \cos\theta\sin\varphi\,\mathbf{u}_\theta + \cos\varphi\,\mathbf{u}_\varphi\,. \tag{112}$$

Using (111) and (112) in (104), we obtain

$$\begin{aligned}\mathbf{u}_t &= \sin(\varphi - \psi)\sin\theta\,\mathbf{u}_r \\ &\quad + \sin(\varphi - \psi)\cos\theta\,\mathbf{u}_\theta + \cos(\varphi - \psi)\,\mathbf{u}_\varphi\,.\end{aligned} \tag{113}$$

In Section IV.B, we have $\mathbf{R}_0 \simeq \mathbf{u}_r$ because $r \gg a$. Accordingly, it follows from (113) that $\mathbf{u}_t \times \mathbf{R}_0$ satisfies (53) and that $-\mathbf{R}_0 \times (\mathbf{R}_0 \times \mathbf{u}_t)$ satisfies (54). We also have

$$\begin{aligned}\overrightarrow{\mathrm{PQ}} &= -a\cos\psi\mathbf{u}_x - a\sin\psi\mathbf{u}_y + r\mathbf{u}_r \\ &= [r - a\sin\theta\cos(\varphi - \psi)]\mathbf{u}_r \\ &\quad + a\cos\theta\cos(\varphi - \psi)\mathbf{u}_\theta + a\sin(\varphi - \psi)\mathbf{u}_\varphi\,,\end{aligned} \tag{114}$$

in which we have used (111) and (112). It follows that

$$R = ||\overrightarrow{\mathrm{PQ}}|| \simeq r - a\sin\theta\cos(\varphi - \psi) \tag{115}$$

because $r \gg a$. We have proven (55).

Finally, we note that, by (109) and (110), on the axis of the loop, where $\theta = 0$ or $\theta = \pi$, we have

$$\cos\theta\sin\varphi\,\mathbf{u}_\theta + \cos\varphi\,\mathbf{u}_\varphi = \mathbf{u}_y \tag{116}$$

and

$$\cos\varphi\,\mathbf{u}_\theta - \cos\theta\sin\varphi\,\mathbf{u}_\varphi = \cos\theta\mathbf{u}_x = \pm\mathbf{u}_x\,, \tag{117}$$

where the plus sign applies to $z > 0$ and the minus sign to $z < 0$. These results are useful to interpret (65)–(66).

## APPENDIX B

This appendix is about reception by the loop antenna.

The results presented in [40, Sec. IV-Sec. V] and [41, Sec. IV] being applicable to a planar wire loop antenna without terminal-zone network, they can be directly used to determine the electromotive force at the gap of the loop antenna, denoted by $e_{gap}$.

According to Fig. 2 and [40, Eq. (73)], we have:

$$e_{gap} = j\omega\mu \iint_{\mathcal{A}} \mathbf{H}_i \cdot \mathbf{u}_z \, d\mathcal{A} - a \int_0^{2\pi} \frac{i_E(\psi) - i_E(0)}{i_E(0)} \, \mathbf{u}_t \cdot \mathbf{E}_i \, d\psi \,, \quad (118)$$

which is equivalent to

$$e_{gap} = -a \int_0^{2\pi} \frac{i_E(\psi)}{i_E(0)} \, \mathbf{u}_t \cdot \mathbf{E}_i \, d\psi \,. \quad (119)$$

According to Fig. 2, we have

$$I_0 = i_E(0) \left( 1 + \frac{j\omega C_T}{Y_\delta} \right) \quad (120)$$

during emission, and the open-circuit voltage of the loop antenna (during reception) is given by

$$e_{ant} = \frac{e_{gap}}{1 + \dfrac{j\omega C_T}{Y_\delta}} \,. \quad (121)$$

It follows from (119)–(121) that

$$e_{ant} = -a \int_0^{2\pi} \frac{i_E(\psi)}{I_0} \, \mathbf{u}_t \cdot \mathbf{E}_i \, d\psi \,, \quad (122)$$

which is equivalent to

$$e_{ant} = j\omega\mu \iint_{\mathcal{A}} \mathbf{H}_i \cdot \mathbf{u}_z \, d\mathcal{A} - a \int_0^{2\pi} \frac{i_E(\psi) - I_0}{I_0} \, \mathbf{u}_t \cdot \mathbf{E}_i \, d\psi \,. \quad (123)$$

These formulas are identical to (84)–(85), though they were derived differently.

## REFERENCES


[1] R.F. Harrington, *Time-Harmonic Electromagnetic Fields*, New York, NY, USA: McGraw-Hill, 1961.

[2] R.E. Collin, *Antennas and Radiowave Propagation*, International Edition, New York, NY, USA: McGraw-Hill, 1985.

[3] T.T. Wu, "Theory of the thin circular loop antenna," *J. Mathematical Physics*, J. Mathematical Physics, vol. 3, no. 6, pp. 1301-1304, 1962.

[4] R.W.P. King, C.W. Harrison, Jr. and D.G. Tingley, "The admittance of bare circular loop antennas in a dissipative medium," *IEEE Trans. Antennas Propagat.*, vol. AP-12, no. 4, pp. 434-438, Jul. 1964.

[5] R.W.P. King, C.W. Harrison, Jr. and D.G. Tingley, "The current in bare circular loop antennas in a dissipative medium," *IEEE Trans. Antennas Propagat.*, vol. AP-13, no. 4, pp. 529-531, Jul. 1965.

[6] R.W.P. King, *Tables of Antenna Characteristics*, New York, NY, USA: IFI Plenum Data Corporation, 1971.

[7] R.W.P. King, "The loop antenna for transmission and reception," ch. 11 of *Antennas Theory, Part 1*, R.E. Collin and F.J. Zucker, Ed., New York, NY, USA: McGraw-Hill, 1969.

[8] E. Jahnke, F. Emde and F. Lösch, *Tables of Higher Functions*, 6th Edition, Stuttgart, Germany: B.G. Teubner Verlagsgesellschaft, 1960.

[9] M. Abramowitz and I.A. Stegun, *Handbook of Mathematical Functions*, New York: Dover, 1965.

[10] F.W.J. Olver, D.W. Lozier, R.F. Boisvert and C.W. Clark, *NIST Handbook of Mathematical Functions*, New York, NY, USA: Cambridge University Press, 2010.

[11] R.W.P. King, *The Theory of Linear Antennas*, Cambridge, MA, USA: Harvard University Press, 1956.

[12] R.W.P. King, R.B. Mack and S.S. Sandler, *Arrays of Cylindrical Dipoles*, London, U.K.: Cambridge University Press, 1968.

[13] H. Jasik, "Fundamentals of antennas," ch. 2 of *Antenna Engineering Handbook*, 3rd ed., R.C. Johnson, Ed., New York, NY, USA: McGraw-Hill, 1993.

[14] G.S. Smith, "Loop antennas," ch. 5 of *Antenna Engineering Handbook*, 3rd ed., R.C. Johnson, Ed., New York, NY, USA: McGraw-Hill, 1993.

[15] G. Zhou and G.S. Smith, "An accurate theoretical model for the thin-wire circular half-loop antenna," *IEEE Trans. Antennas Propagat.*, vol. 39, no. 8, pp. 1167-1177, Aug. 1991.

[16] H.T. Anastassiou, "Fast, simple and accurate computation of the currents on an arbitrarily large circular loop antenna," *IEEE Trans. Antennas Propagat.*, vol. 54, No. 3, pp. 860-866, Mar. 2006.

[17] H.T. Anastassiou, "Input susceptance of an arbitrarily large, circular loop antenna," *Proc. First European Conf. on Antennas and Propagation, EuCAP 2006*, Nice, France, pp. 1-5, Nov. 2006.

[18] J.D. Kraus, *Antennas*, First Edition, New York, NY, USA: McGraw-Hill, 1950.

[19] E. Ramis, C. Deschamps and J. Odoux, *Cours de mathématiques spéciales — 3 — Topologie et éléments d'analyse*, 3rd ed., Paris, France: Masson, 1991.

[20] C.T.A Johnk, *Engineering Electromagnetic Fields and Waves*, New York, NY, USA: John Wiley & Sons, 1975.

[21] L.W. Rispin and D.C. Chang, "Wire and loop antennas," ch. 7 of *Antennas Handbook — Volume II — Antenna theory*, Y.T. Lo and S.W. Lee, Ed., New York, NY, USA: Van Nostrand Reinhold, 1993.

[22] K. Iizuka, R.W.P. King and C.W. Harrison, Jr., "Self- and mutual admittances of two identical circular loop antennas in a conducting medium and in air," *IEEE Trans. Antennas Propagat.*, vol. AP-14, no. 4, pp. 440-450, Jul. 1966.

[23] R.F. Harrington, *Field Computation by Moment Methods*, Piscataway, NJ, USA: IEEE Press, 1993.

[24] J.E. Storer, "Impedances of thin-wire loop antennas," *Trans. of the American Institute of Electrical Engineers, Part I: Communication and Electronics*, vol. 75, no. 5, pp. 606-619, Nov. 1956.

[25] J.A. Stratton, *Electromagnetic Theory*, New York, NY, USA: McGraw-Hill, 1941.

[26] S.J. Orfanidis, *Electromagnetic Waves and Antennas — vol. 2 — Antennas*, Sophocles J. Orfanidis, 2016.

[27] J.D. Kraus, *Electromagnetics*, Fourth Edition, New York, NY, USA: McGraw-Hill, 1992.

[28] D.H. Werner, "An exact integration procedure for vector potentials of thin circular loop antennas," *IEEE Trans. Antennas Propag.*, vol. 44, no. 2, pp. 157-165, Feb. 1996.

[29] D.H. Werner, "Correction to 'An exact integration procedure for vector potentials of thin circular loop antennas'," *IEEE Trans. Antennas Propag.*, vol. 44, no. 8, p. 1199, Aug. 1996.

[30] L.-W. Li, M.-S. Leong, P.-S. Kooi and T.-S. Yeo, "Exact solutions of electromagnetic fields in both near and far zones radiated by thin circular-loop antennas: A general representation," *IEEE Trans. Antennas Propag.*, vol. 45, no. 12, pp. 1741-1748, Dec. 1997.

[31] D.H. Werner, "Comments on 'Exact solutions of electromagnetic fields in both near and far zones radiated by thin circular-loop antennas: A general representation'," *IEEE Trans. Antennas Propag.*, vol. 49, no. 1, p. 109, Jan. 2001.

[32] L.-W. Li, "Reply to 'Comments on "Exact solutions of electromagnetic fields in both near and far zones radiated by thin circular-loop antennas: A general representation"'," *IEEE Trans. Antennas Propag.*, vol. 49, no. 1, pp. 109-110, Jan. 2001.

[33] J.T. Conway, "New exact solution procedure for the near fields of the general thin circular loop antenna," *IEEE Trans. Antennas Propag.*, vol. 53, no. 1, pp. 509-517, Jan. 2005.

[34] S.M.A. Hamed, "Exact field expressions for circular loop antennas using spherical functions," *IEEE Trans. Antennas Propag.*, vol. 61, no. 6, pp. 2956-2963, Jun. 2013.
[35] K.H.R. Zheng and J.L.-W. Li, "Comments on 'Exact field expressions for circular loop antennas using spherical functions expansion'," *IEEE Trans. Antennas Propag.*, vol. 62, no. 8, pp. 4432-4434, Aug. 2014.
[36] S.M.A. Hamed, "Response to 'Comments on "Exact field expressions for circular loop antennas using spherical functions expansion"'," *IEEE Trans. Antennas Propag.*, vol. 62, no. 8, pp. 4434-4435, Aug. 2014.
[37] D.G. Miljak, "Exact expressions for the near field of a thin uniform circular loop current with application to loops lying on a half space," *Progress In Electromagnetics Research B*, vol. 105, pp. 93-105, Mar. 2024.
[38] D.H. Werner, "Exact expressions for the far-zone electromagnetic fields radiated by thin elliptical loop antennas of arbitrary size," *IEEE Trans. Antennas Propag.*, vol. 66, no. 12, pp. 6844-6850, Dec. 2018.
[39] C.A. Balanis, *Antenna Theory*, 2nd ed., New York, NY, USA: John Wiley & Sons, 1997.
[40] F. Broydé and E. Clavelier, "The Open-Circuit Voltage of a Planar Wire Loop Antenna Used for Reception," *Excem Research Papers in Electronics and Electromagnetics*, no. 6, doi: 10.5281/zenodo.7498910, Jan. 2023.
[41] F. Broydé and E. Clavelier, "Contribution to the theory of planar wire loop antennas used for reception," *IEEE Trans. Antennas Propag.*, vol. 68, no. 3, pp. 1953-1961, Mar. 2020.
[42] E.C. Jordan and K.G. Balmain, *Electromagnetic Waves and Radiating Systems*, 2nd ed., Englewood Cliffs, NJ, USA: Prentice-Hall, 1968.
[43] R.E. Collin, "The receiving antenna," ch. 4 of *Antennas Theory, Part 1*, R.E. Collin and F.J. Zucker, Ed., New York, NY, USA: McGraw-Hill, 1969.
[44] F.E. Terman, *Radio Engineers' Handbook*, New York, NY, USA: McGraw-Hill, 1943.
[45] R. Keen, *Wireless Direction Finding*, Third and Enlarged Edition, London, U.K.: Iliffe & Sons Limited, 1938.
[46] D.S. Bond, *Radio Direction Finders*, First Edition, New York, NY, USA: McGraw-Hill, 1944.
[47] H.D. Kennedy and R.B. Woolsey, "Direction-finding antennas," ch. 39 of *Antenna Engineering Handbook*, 3rd ed., R.C. Johnson, Ed., New York, NY, USA: McGraw-Hill, 1993.
[48] H. Whiteside and R.W.P. King, "The loop antenna as a probe," *IEEE Trans. Antennas Propag.*, vol. AP-12, no. 3, pp. 291-297, May 1964.

FRÉDÉRIC BROYDÉ was born in France in 1960. He received the M.S. degree in physics engineering from the Ecole Nationale Supérieure d'Ingénieurs Electriciens de Grenoble (ENSIEG) and the Ph.D. in microwaves and microtechnologies from the Université des Sciences et Technologies de Lille (USTL).

He co-founded the Excem corporation in May 1988, a company providing engineering and research and development services. He is president of Excem since 1988. He is now also president of Eurexcem, a subsidiary of Excem. Most of his activity is allocated to research in electronics, radio, antennas, electromagnetic compatibility (EMC) and signal integrity.

Dr. Broydé is author or co-author of about 100 technical papers, and inventor or co-inventor of about 90 patent families. He is a Senior Member of the IEEE since 2001. He is a licensed radio amateur (F5OYE).

EVELYNE CLAVELIER was born in France in 1961. She received the M.S. degree in physics engineering from the Ecole Nationale Supérieure d'Ingénieurs Electriciens de Grenoble (ENSIEG).

She is co-founder of the Excem corporation, based in Maule, France, and she is currently CEO of Excem. She is also president of Tekcem, a company selling or licensing intellectual property rights to foster research. She is an active engineer and researcher.

Her current research areas are radio communications, antennas, matching networks, EMC and circuit theory.

Prior to starting Excem in 1988, she worked for Schneider Electrics (in Grenoble, France), STMicroelectronics (in Grenoble, France), and Signetics (in Mountain View, CA, USA).

Ms. Clavelier is the author or a co-author of about 90 technical papers. She is co-inventor of about 90 patent families. She is a Senior Member of the IEEE since 2002. She is a licensed radio amateur (F1PHQ).

•••